Journal of Controlled Release 235 (2016) 379–392

Contents lists available at ScienceDirect

Journal of Controlled Release

journal homepage: www.elsevier.com/locate/jconrel

Substitution of blood coagulation factor X-binding to Ad5 by position-specific PEGylation: Preventing vector clearance and preserving infectivity

L. Krutzke [a], J.M. Prill [a], T. Engler [a], C.Q. Schmidt [b], Z. Xu [c], A.P. Byrnes [c], T. Simmet [b], F. Kreppel [a,*]

[a] Department of Gene Therapy, Ulm University, Ulm, Germany
[b] Institute of Pharmacology of Natural Products and Clinical Pharmacology, Ulm University, Ulm, Germany
[c] Division of Cellular and Gene Therapies, Center for Biologics Evaluation and Research, Food and Drug Administration, Silver Spring, MD, USA

ARTICLE INFO

Article history:
Received 9 March 2016
Received in revised form 9 June 2016
Accepted 10 June 2016
Available online 11 June 2016

Keywords:
Adenovirus
Blood coagulation factor X
PEG
Natural antibodies
Pharmacokinetics

ABSTRACT

The biodistribution of adenovirus type 5 (Ad5) vector particles is heavily influenced by interaction of the particles with plasma proteins, including coagulation factor X (FX), which binds specifically to the major Ad5 capsid protein hexon. FX mediates hepatocyte transduction by intravenously-injected Ad5 vectors and shields vector particles from neutralization by natural antibodies and complement. In mice, mutant Ad5 vectors that are ablated for FX-binding become detargeted from hepatocytes, which is desirable for certain applications, but unfortunately such FX-nonbinding vectors also become sensitive to neutralization by mouse plasma proteins. To improve the properties of Ad5 vectors for systemic delivery, we developed a strategy to replace the natural FX shield by a site-specific chemical polyethylene glycol shield. Coupling of polyethylene glycol to a specific site in hexon hypervariable region 1 yielded vector particles that were protected from neutralization by natural antibodies and complement although they were unable to bind FX. These vector particles evaded macrophages *in vitro* and showed significantly improved pharmacokinetics and hepatocyte transduction *in vivo*. Thus, site-specific shielding of Ad5 vectors with polyethylene glycol rendered vectors FX-independent and greatly improved their properties for systemic gene therapy.

1. Introduction

Recombinant adenovirus vectors, in particular type 5 (Ad5), are frequently used for gene therapy. However, successful systemic delivery of Ad5-based gene transfer vectors is limited by complex interactions of the vector with multiple cellular and non-cellular host blood components. These interactions result in rapid sequestration of >90% of the vector particles by the reticuloendothelial system [1]. The sequestration is caused by opsonization of vector particles due to binding of antibodies [2–5] and complement components [6,7], uptake of particles by liver sinusoidal endothelial cells (LSEC) [1] and liver residential Kupffer cells (KC) [8–11], and transduction of hepatocytes [12,13]. Furthermore, in humans and rats Ad5 particles are trapped by erythrocytes [14–16].

Macrophages represent a major sink for i.v. injected vector particles and contribute to rapid clearance of the vector from blood [8,17], Ad-induced toxicity [18,19] and limited transduction of target tissues [6,20]. The uptake of Ad5 vector particles by macrophages is mainly mediated by scavenger receptor-A (SR-A) and scavenger receptor expressed on endothelial cells-I (SREC-I) [6,17,21–23]. Scavenger receptors can bind negatively charged molecules [22] and Ad5 vector particles have a net negative surface charge that is mainly located in the hypervariable regions (HVRs) of the hexon protein [8,24–27].

In addition to the vector's intrinsic charge pattern, the interaction of the particles with host blood coagulation factor X (FX) plays a pivotal role for the biodistribution of Ad5. Blood coagulation FX binds to distinct amino acid residues in the HVRs of hexon [28]. *In vitro* it was shown that capsid-bound FX can mediate transduction of hepatocytes [12] by bridging the particles to heparan sulfate proteoglycans (HSPGs) [29]. Importantly, recent findings in mice demonstrated that mutant Ad5 vectors that are unable to bind FX become opsonized and neutralized by natural IgM antibodies and the classical complement pathway [5]. This finding indicates that capsid-bound FX provides a shield from complement and natural antibodies. Both natural antibodies and complement can contribute to the sequestration of Ad5 vector particles by KC. Xu et al. reported a modest increase in vector uptake by Kupffer cells upon depletion of vitamin-K-dependent coagulation factors by warfarin pretreatment of mice [6]. Alba et al. demonstrated increased Ad5 genome accumulation in liver and spleen 1 h after injection of FX-binding ablated Ad5 vectors [30]. In sum, the fate of FX binding-ablated vectors remains largely elusive, to our knowledge there are no studies available to date that examine the effects of FX on the

* Corresponding author.
E-mail address: florian.kreppel@uni-ulm.de (F. Kreppel).

http://dx.doi.org/10.1016/j.jconrel.2016.06.022

pharmacokinetics of vector particles. Overall, current data suggest that mutating the Ad5 capsid to modify its interactions with FX can have unintended effects on vector activity *in vivo*, and that a more sophisticated strategy is needed to improve pharmacokinetic profiles. Therefore, we sought to generate vectors that do not bind FX yet are still shielded from neutralization by natural antibodies and complement.

Many attempts have been made to avoid detrimental vector-host interactions by modifying the vector capsid either genetically or chemically. The success of genetic modifications is often limited by structural constraints of the vector particles. Moreover, genetic modifications can typically be employed at only a few sites of the capsid and thus it is difficult to address multiple complex vector-host interactions solely by genetic means. As an alternative, vectors can be chemically modified with synthetic polymers that non-specifically shield the capsid as a whole. Such cloaked vectors show improved pharmacokinetics but can exhibit reduced vector infectivity due to the extensive 'wrapping' [8,31–35]. These shortcomings emphasize the need for new modification strategies in order to generate re-targeted Ad5 vector particles suitable for i.v. delivery.

To this end, we generated Ad5 vectors with a genetically introduced cysteine residue in the hypervariable region 1 (HVR1) of hexon, which enabled position-specific covalent attachment of only up to 720 maleimide-activated polyethylene glycol shielding polymers [36]. In addition to this minimal geneti-chemical modification, the vectors carried point mutations in the fiber knob domain (ΔCAR) to inhibit binding to the natural coxsackie and adenovirus receptor (CAR) [37], and in hexon HVR7 (ΔFX) to inhibit binding of blood coagulation factor X [28]. Finally, by position-specific coupling of polyethylene glycol (PEG) moieties to HVR1 we aimed to provide a shield to evade complement- and natural antibody-mediated neutralization. We hypothesized that the position-specific PEGylation might shield the negative charges of HVR1 and therefore might limit charge-mediated vector sequestration *via* scavenger receptors [8,24].

In summary, the position-specific PEGylation of HVR1 preserved the infectivity of the vector particle, prevented complement- and natural antibody-mediated neutralization, and ablated scavenging of the particles through scavenger receptor-dependent mechanisms. Furthermore, depending on the PEG size, PEGylation improved the pharmacokinetic profile and increased transduction of hepatocytes, thus rendered particles independent of the natural FX shield.

2. Material and methods

2.1. Cell lines and cell culture

A549 cells (ATCC #CCL-243) were cultivated in MEM (Gibco, Carlsbad, CA). SKOV-3 cells (ATCC #HTB-77) were cultivated in RPMI (Gibco, Carlsbad, CA). Raw264.7 cells (ATCC #TIB-71) were cultivated in RPMI (Gibco, Carlsbad, CA). J774A.1 (ATCC #TIB-67) cells were cultivated in DMEM (Gibco, Carlsbad, CA). Hepa1–6 (ATCC #CRL-1830) and N52.E6 cells [38] were cultivated in α-MEM (Gibco, Carlsbad, CA). All cell culture media were supplemented with 10% fetal calf serum (for SKOV-3 cells only 5%) and 1% penicillin/streptomycin/glutamine (Gibco, Carlsbad, CA). Cells were passaged twice a week.

2.2. Adenovirus vectors

Vectors used in this study were *E1*-deleted first generation vectors of human adenovirus type 5 (based on GenBank AY339865.1, sequence from nt 1 to 440 and from nt 3523 to 35935). Vector genomes carried a human CMV promoter-driven *EGFP* expression cassette subcloned from pEGFP-N1 (Clontech). Point mutations were introduced using Red/ET-based homologous recombination (GeneBridges, Heidelberg, Germany) in electrocompetent *Escherichia coli* (ElectroMAX™ DH10B ™, Invitrogen, Karlsruhe, Germany). To inhibit the binding of vector particles to CAR, a point mutation within the fiber knob was introduced (Protein ID: AAQ19310.1; tyrosine at position 477 was exchanged for alanine; sequence: NNSFLDPEAWNFRNGDL; designation: ΔCAR), as described previously [37]. To inhibit the binding of vector particles to FX, a point mutation within HVR7 of the hexon protein was introduced (Protein ID: AAQ19298.1; glutamic acid at position 451 was exchanged for glutamine; sequence: ATEFSDKNQIRVGNNFA; designation: ΔFX), as described previously [28]. To induce a chemical reactivity for position-specific PEGylation, a cysteine residue was introduced into HVR1 of hexon (Protein ID: AAQ19298.1; aspartic acid at position 151 was exchanged for cysteine; sequence: EINLEEEDCDNEDEVDE; designation: HVR1).

2.3. Adenovirus vector purification

Ad5 vectors were propagated in N52.E6 cells which transcomplement *E1* [38]. Cells were infected with physical multiplicity of infection (pMOI) 500 and harvested 48 h p.i. Vector purification by CsCl gradient centrifugation was performed as previously described [36,39]. For cysteine-carrying vectors, lysis buffers contained 5 mM and discontinuous gradient buffers contained 1 mM TCEP (Invitrogen, Karlsruhe, Germany) as reducing reagent to prevent aggregation of particles due to oxidation of cysteines [36]. To purify PEGylated vector particles, two consecutive discontinuous CsCl gradients were performed; only the first discontinuous gradient buffer was supplemented with 1 μM TCEP. All buffers were degased and argon-saturated.

Physical titers were determined by either optical density at 260 nm, after vector lysis with 0.5% sodium dodecyl sulfate and heating at 56 °C for 10 min [40] or by DNA-based slot-blot procedure [41].

2.4. PEGylation of vector capsids

Different sizes (2 kDa, 5 kDa, 20 kDa) of the maleimide-activated linear polymer PEG (MeO-PEG-mal; IRIS Biotech Marktredwitz, Germany) were used in a 20-fold molar excess over cysteines of purified vector particles. Immediately before mixing with vectors, PEG moieties were dissolved in a 50 mM HEPES buffer, pH 7.2. Vector:PEG solutions were incubated for 1 h at room temperature, rotating. Subsequently, samples were purified by discontinuous CsCl gradient centrifugation to remove uncoupled PEG moieties.

2.5. Visualization of proteins by silver staining after SDS-PAGE

1×10^{10} vector particles were mixed with SDS-loading buffer, heated for 5 min at 70 °C and loaded on an 8% separation/5% stacking SDS gel, running at 80 V. Silver staining of separated vector proteins was done as previously described [42].

2.6. Transduction assays

Transduction assays were performed using A549 cells, Hepa1–6 cells or SKOV-3 cells. 2×10^4 cells/well were seeded on coated, flat bottom 96-well plates (NUNC, Langenselbold, Germany) and cultivated overnight. The following day cells were washed with PBS, and supplemented with 100 μl serum-free medium containing no or 8 μg/ml of human FX (CellSystems Biotechnologie, Troisdorf, Germany). Cells were transduced with pMOI 1000 in triplicates, incubated for 3–4 h at 37 °C, washed with PBS and 200 μl serous medium was added. Cells were incubated for 24 h (for SKOV-3 cell 72 h), harvested and EGFP expression was analyzed by flow cytometry (Beckman Coulter Gallios Flow Cytometer).

2.7. Real-time quantitative PCR analysis

DNA samples were analyzed for their vector DNA content by quantitative real time PCR of the *E4* region of the vector genome and normalization using *β-actin* copy numbers. Therefore 10 μl of Kapa SYBR FAST

qPCR Universal Master Mix (PEQLAB Biotechnologie, Erlangen, Germany), 0.4 μl of 10 pmol/μl primer forward and reverse (for *E4*: forward 5′-tagacgatccctactgtacg-3′; reverse 5′-ggaaatatgactacgtccgg-3′; for murine *β-actin*: forward 5′-caaggagtgcaagaacacag-3′; reverse 5′-gccttggagtgtgtattgag-3′; for human *β-actin*: forward 5′-gctcctcctgagcgcaag-3′; reverse 5′-catctgctggaaggtggaca-3′) and 2 μl sample were mixed in a final volume of 20 μl.

PCR cycles were performed as follows: 1 cycle: 10 min 95 °C (denaturation); 40 cycles: 30 s 95 °C (denaturation) — 30 s 60 °C (annealing) — 20 s 72 °C (elongation).

2.8. Surface plasmon resonance analysis

Surface plasmon resonance analysis was performed using a SR7500DC Dual Channel Surface Plasmon Resonance Spectrometer (Reichert Technologies Life Sciences, Buffalo, NY, USA) at 25 °C. Human FX was coated on a carboxymethyldextran hydrogel-coated CMD500m gold chip with a medium carboxylate density and a max. capacity of 40.000 response units (RU) (XanTec bioanalytics GmbH, Düsseldorf, Germany). After repeated injections of running buffer (10 mM HEPES, 150 mM NaCl, 5 mM $CaCl_2$, 0.005% Tween20, pH 7.4) at a flowrate of 25 μl/min at 25 °C for 10 min, the left and right surfaces were activated by flowing a 1:1 mixture of 0.1 M 1-Ethyl-3-(3-dimethylaminopropyl)carbodiimid and 0.1 M Sulfo-NHS in 5 mM MES buffer pH 6 at a flowrate of 25 μl/min for 4 min. Subsequently, 59 μg/ml FX diluted in 5 mM NaAc buffer, pH 4.9 were injected onto the left surface only, at a flowrate of 10 μl/min for 5 min. Uncoated carboxyl groups were quenched by injection of 1 M ethanolamine, pH 8.5 onto both surfaces at a flowrate of 25 μl/min for 4 min. The right surface (which was only activated and quenched in absence of a ligand) served as the reference surface *i.e.* the reference signals from the right surface were subtracted from the signals achieved on the FX-surface (left) to achieve reference subtracted responses. Glycerol of vector particle solutions was removed using PD MiniTrap G-25 columns (Amersham, Buckinghamshire, UK) according to the manufacturer but without filter. Vectors were diluted in running buffer, supplemented with TCEP in a 10-fold molar excess over cysteine and Ca^{2+} concentrations were adjusted to 5 mM. Different vector dilution series were injected (single values or duplicates; 1×10^9 VP/μl; 1×10^9 VP/μl; 5×10^8 VP/μl; 5×10^8 VP/μl; 2.5×10^8 VP/μl; 1.25×10^8 VP/μl) at a flowrate of 25 μl/min for 3 min. Each vector injection was followed by injection of regeneration buffer (10 mM HEPES, 150 mM NaCl, 3 mM EDTA, 0.005% Tween20, pH 7.4) at a flowrate of 25 μl/min for 50 s.

Saturation of the FX-coated chip by Ad injection was not reached with the used conditions. Since the quality of the FX surface decreased over time (compare repeated Ad-wtcapsid injections at same concentration S1a–h), Ad-wtcapsid vectors with a concentration of 1×10^9 VP/μl were injected once before each vector dilution series as a reference to determine the binding capacity of the FX surface at different time points. Binding of modified vectors to FX was quantified by normalizing the response of the various modified vectors at concentrations of 1×10^9 VP/μl to the measured response of the reference Ad-wtcapsid vector, which had been injected immediately before.

2.9. ZetaSizer measurement

2×10^{11} VP were diluted in 1 ml buffer (50 mM HEPES, 0.1 mM DTT, pH 7.4). Glycerol of vector particle solutions was removed using PD MiniTrap G-25 columns (Amersham, Buckinghamshire, UK) according to the manual but without filter. Vector solutions were injected in a clear disposable zeta cell (DTS1070, Malvern, Worcestershire, UK). The zeta potential was measured using a ZetaSizer Nano-ZS (Malvern, Worcestershire, UK) at 25 °C and analyzed with DTSNano 5.10 software.

2.10. Vector binding to human blood cells

1×10^8 VP diluted in PBS ± 10 mg/ml human intravenous IgG (IVIG, Privigen, CSL Behring, Marburg, Germany) in a final volume of 100 μl were incubated for 30 min at 37 °C rotating with 200 μl human whole blood of three healthy donors, ELISA-tested to be Ad-naïve. Blood was *anti*-coagulated with 50 μg/ml Lepirudin (Celgene, Windsor, UK) to preserve complement activity. Subsequently, cells and plasma were separated by centrifugation for 10 min at 500 ×*g*. 20 μl of each fraction were diluted in PBS in a final volume of 200 μl.

To identify the blood cell type to which the vector particles were attached, 20 ml of ELISA-tested *anti*-Ad IgG-positive hirudinized human whole blood were incubated with 1×10^{10} Ad-HVR1 vector particles in a final volume of 30 ml for 30 min at 37 °C rotating. Subsequently, blood samples were carefully layered onto 5 ml bicoll separation solution (Biochrom, Berlin, Germany) and plasma, leukocytes and erythrocytes were separated by centrifugation for 30 min at 500 ×*g* at 20 °C without brake. Plasma and blood cells were isolated and cells were washed twice with 10 ml PBS. 20 μl plasma, 1×10^5 leukocytes or 6.7×10^7 erythrocytes were diluted in PBS in a final volume of 200 μl each.

The DNA of all samples was isolated using GenElute Mammalian Genomic DNA miniprep Kit (Sigma-Aldrich, Steinheim, Germany), and stored at −80 °C in 10 mM Tris buffer pH 8.0. The Ad5 genome content of the samples was determined by qPCR analysis and normalized using human *β-actin* copy numbers. β-*actin* was detectable in the plasma samples prepared as described above and thus exploited for normalization.

2.11. Animals

Female BALB/c mice at the age of 8–10 weeks were used to analyze pharmacokinetics and liver transduction. Animals (received from Charles River, Sulzfeld, Germany) were maintained in pathogen-free, individually ventilated cages (Tecniplast, Hohenpreissenberg, Germany) and fed with sterilized diet for laboratory rodents (Ssniff, Soest, Germany). All experiments were in accordance with policies and procedures of institutional guidelines and approved by the Animal Care Commission of the Government Baden-Württemberg or the FDA Center for Biologics Evaluation and Research Animal Care and Use Committee. For fluorometic analysis of the liver also antibody-deficient J_HD [43] mice on BALB/c background were bred at FDA. Whole blood samples of the strains C57BL/6, NMRI, BALB/c or antibody-deficient *muMT*−/− (B6. 129S2-*Igh*-6^{tm1Cgn}/J; JAX Mice Database: 002288) mice were a kind gift of neighboring working groups of Ulm University. *muMT*−/− mice were developed by disruption of an exon of the immunoglobulin heavy chain of the IgM antibody class. Mice are lacking mature B cells and have almost undetectable serum levels of IgG1, IgG2a, IgG2b, IgG3, IgM and IgA. Blood samples were anticoagulated using 50 μg/ml Lepirudin (Celgene Europe Ltd., Windsor, UK). Plasma samples was prepared by pelleting the cells for 10 min at 500 ×*g*.

2.12. Pharmacokinetics

BALB/c mice were anesthetized by intraperitoneal injection of 150 mg/kg ketamine and 30 mg/kg xylazine. 2×10^{10} VP diluted in PBS in a final volume of 200 μl, were injected into the dorsal tail vein of mice. After 2, 4, 6, 10 and 20 min small blood samples of 20 μl were collected in heparinized glass capillaries from the lateral tail veins by snipping the tail. Samples were mixed with PBS in a final volume of 200 μl. Genomic DNA of samples was extracted using GenElute Mammalian Genomic DNA Miniprep Kit (Sigma-Aldrich, Steinheim, Germany), and stored at −80 °C in 10 mM Tris buffer pH 8.0. To analyze blood cell association, 100 μl whole blood was collected by puncturing the heart at 20 min p.i. Samples were centrifuged at 800 ×*g* for 10 min, supernatants discarded, and cells were resuspended in a final

volume of 200 μl PBS before the DNA was isolated. The vector DNA content of all samples was determined by qPCR analysis and normalized using murine β-*actin* copy numbers. Calculations of area under the curve (AUC) between 2 min and 20 min were done using SciDAVis 1.D5 software (integration by linear interpolation for curve fitting).

2.13. Fluorometic analysis of liver homogenates

2×10^{10} VP diluted in PBS in a total volume of 200 μl were injected into the dorsal tail vein of BALB/c mice. Mice were sacrificed 72 h p.i. by isoflurane (Forene, Abbott, Ludwigshafen, Germany) inhalations and subsequent liver perfusion with PBS. Fluorometric analysis of the EGFP expression intensity in the liver tissue was done as previously described [44].

For fluorometic analysis of liver homogenates of J_HD mice, the animals were anesthetized by i.p. injection of 150 mg/kg ketamine and 30 mg/kg xylazine 10 min prior to sacrifice. Livers were harvested and 200 mg tissue were homogenized in 0.4 ml ice-cold lysis buffer (25 mM Tris-phosphate pH 7.6, 2 mM EDTA, 10% Glycerol, 1% Triton X-100, 1/100 protease inhibitor cocktail (Thermo Scientific #1861279)) and 0.8 g of 0.5 mm zirconium oxide beads at speed 10 for 2 min using a bullet blender (Next Advance, Inc.). 100 μl of 1:20 and 1:200 diluted lysate were transferred to a black 96-well flat bottom plate (Greiner Bio One). EGFP fluorescence was measured at 490/510–570 nm with the Blue Optical Kit of Turner Biosystems. Values were expressed as arbitrary units of luminescence per mg protein (AU/mg protein). Protein concentrations of liver lysate were determined by BIO-RAD DC Protein Assay Kit (BIO-RAD Laboratories, Hercules, CA 94547, USA).

2.14. Fluorescence microscopy of liver and spleen sections

Fluorescence microscopy of murine liver and spleen sections were done as previously described [39].

2.15. Uptake by macrophages

1×10^5 cells/well of the murine macrophage cell lines Raw264.1 or J774A.1 were seeded on coated, flat bottom 24-well plates (NUNC, Langenselbold, Germany) and cultivated overnight. The following day, cells were washed with PBS, and supplemented with 500 μl serum-free medium. 2×10^8 vector particles (corresponding to pMOI 2000 in this assay) were pre-incubated in a final volume of 30 μl with PBS or hirudinized (50 μg/ml, dissolved in PBS) plasma with preserved complement activity of either C57BL/6 or antibody-deficient *muMT*−/− mice for 20 min at 37 °C. The complement system of plasma samples was destroyed by heating (56 °C for 30 min). Raw264.7 cells were incubated with the vector:PBS or vector:plasma solution for 2 h at 37 °C. J774A.1 cells were treated or not with 30 μg/ml poly-(I) (Sigma-Aldrich, Steinheim, Germany) for 1 h at 37 °C. Subsequently, J774 cells were incubated with 2×10^8 vector particles (pMOI 2000) for 2 h. J774 cells were washed and incubated for 24 h at 37 °C. Genomic DNA of samples was extracted using GenElute Mammalian Genomic DNA Miniprep Kit (Sigma-Aldrich, Steinheim, Germany). Samples were stored at −80 °C in 10 mM Tris buffer pH 8.0. The vector DNA content of the samples was determined by qPCR analysis and normalized using murine β-*actin* copy numbers.

2.16. Neutralization of vector particles

2×10^4 cells/well A549 were seeded on coated, flat bottom 96-well plates (NUNC, Langenselbold, Germany) and cultivated overnight. The following day, cells were washed with PBS, and supplemented with 100 μl serum-free medium. 2×10^7 vector particles dissolved in 1–2 μl PBS were mixed with 15 μl PBS or hirudinized plasma with preserved complement activity of either C57BL/6, antibody-deficient *muMT*−/− mice or human plasma from healthy donors tested by ELISA to be positive for *anti*-Ad5 IgGs (n = 3) or Ad-naïve (n = 3). The complement system of plasma samples was destroyed by heating (56 °C for 30 min). For titration assays 2×10^7 vector particles dissolved in 1–2 μl PBS were mixed with 1, 2, 5, 10 or 15 μl of C75BL/6 plasma. Cells were transduced with pMOI 1000 and incubated for 24 h. EGFP expression was analyzed by flow cytometry.

2.17. ELISA for C3 detection

96 well flat bottom plates (NUNC-Maxisorp, Langenselbold, Germany) were coated overnight at 4 °C with 3×10^9 VP in 0.2 M carbonate-bicarbonate, pH 9.6 and then blocked with SuperBlock (PBS) Blocking Buffer (Thermo Scientific #37515, Rockford, USA) for 2 h at room temperature. To test the coating efficiency, Ad5 fiber was detected with monoclonal mouse *anti*-Ad5 fiber antibody (1:300; AM00311PU-N, Acris, Herford, Germany) and HRP-conjugated polyclonal rabbit *anti*-mouse antibody (1:1.000; Sigma-Aldrich, A9044, Steinheim, Germany). For C3 ELISAs, plates were incubated with hirudinized murine plasma (diluted 1:5 in PBS with 2% BSA, 0.05% Tween20, 0.5 mM Mg^{2+} and 0.9 mM Ca^{2+}) for 1 h at room temperature. Murine C3b was detected with monoclonal rat *anti*-mouse C3b antibody (1:1.000; Cedarlane Laboratories Ltd., Burlington, Ontario, Canada; clone RmC11H9; detects also C3, iC3b, and C3dg) and HRP-conjugated goat *anti*-rat antibody (1:1.500; Sigma-Aldrich, A9037, Steinheim, Germany). Plates were developed with o-Phenyldiaminedihydrochloride (Sigma, Steinheim, Germany)/H_2O_2 substrate and stopped with 1 M sulfuric acid. Absorbance was measured at 491 nm/620 nm.

2.18. Toxicity assay for IL-6

300 μl hirudinized murine whole blood of C57BL/6 mice was incubated with 4×10^9 VP dissolved in 2 μl PBS for 6 h at 37 °C, rotating. Samples were centrifuged for 10 min at 1.000 ×*g*. The IL-6 concentration in the plasma fraction was determined by OptEIA Mouse IL-6 ELISA Kit (BD Biosciences, 550950, San Jose, CA, USA) according to manufacturer's instructions.

2.19. Ad particle size measurements

Vector particle size was determined with a NanoSight LM10 instrument equipped with a red laser and Allied Vision Technologies camera (NanoSight, Amesbury, UK). Settings were used according to Kramberger et al. 2012 (except: brightness = 0) [45]. PCS Control L100 (Beckman Coulter, Fullerton, CA) Latex beads with a diameter of 100 nm and a concentration of 1.4×10^6 beads/μl were used as quality control. Vectors were diluted in 50 mM HEPES, 10 mM TCEP buffer pH 7.2 to a final concentration of 1.5×10^6 to 1.9×10^6 particles/μl. Buffers were filtered (0.2 μm), degased and argon-saturated before use. 300 μl of the vector samples were injected into the LM10 unit using a sterile syringe. Sample videos were recorded for 60 s and analyzed with the Nanoparticle Tracking and Analysis (NTA) 2.3 software. The temperature was measured with an OMEGA HH804 device (Omega Engineering, Stanford, CA, USA).

2.20. Statistics

Results are given as mean ± standard deviation. Statistical analysis was performed using unpaired two-sample (Welch) student's *t*-test. Calculations were done with RStudio-software Version 2.15.0 [46]. P-values ≤ 0.05 were considered statistically significant. Calculations of AUC-values were done using SciDAVis 1.D5 software (integration by linear interpolation for curve fitting).

3. Results

3.1. Physical and biological characterization of geneti-chemically modified vector particles

We generated EGFP-expressing Δ*E1* first-generation Ad5 vectors carrying three different point mutations to analyze interactions of Ad5 with cellular and non-cellular blood components *in vitro* and *in vivo*. The first point mutation (ΔCAR; fiber Y477A) reduced binding of the vector particles to their primary receptor CAR. The second mutation (ΔFX; hexon HVR7 E451Q) inhibited binding of blood coagulation factor X to hexon, and the third mutation (HVR1; hexon HVR1 D151C) introduced the chemical reactivity for position-specific PEGylation in form of a thiol group (Table 1). Vectors were PEGylated with maleimide-activated thiol-reactive PEG moieties of different sizes (2000 Da (2K), 5000 Da (5K) and 20,000 Da (20K)) and purified by CsCl gradient centrifugation to remove uncoupled PEG. Coupling efficiency and specificity were determined by SDS-PAGE and silver staining, and the results confirmed a near-quantitative PEGylation of the monomeric hexon (for representative staining see Fig. 1a). Thus, vector particles were modified with ~700 PEG moieties/particle at defined positions.

We performed extensive biophysical characterization of the vector particles to analyze the influence of PEGylation on surface charges and particle sizes. Zeta potential measurements revealed that neither the introduced cysteine nor the ΔFX mutation altered the surface charge of particles compared to an Ad-wtcapsid vector (Fig. 1b). However, PEGylation significantly reduced the negative surface charge of the particles in a PEG size-dependent manner (unPEG: -37 ± 1.8 mV; 2K-PEG: -26 ± 1.1 mV, $p < 1.1 \times 10^{-5}$; 5K-PEG: -23 ± 2.5 mV, $p < 1.6 \times 10^{-5}$; 20K-PEG: -7 ± 0.9 mV, $p < 6.1 \times 10^{-8}$). NanoSight measurements revealed an increase of the hydrodynamic particle diameter by up to 20%, which was positively correlated with the PEG size (Table 2). *In vitro* transduction assays in CAR-expressing A549 cells showed that neither the ΔFX mutation nor the introduced cysteine ablated the ability of the vectors to transduce cells *via* CAR (Fig. 1c). In contrast and as expected, the ΔCAR mutation reduced transduction by approximately 100-fold (Fig. 1c). Importantly, PEGylation of HVR1 with PEG moieties ≤5K did not reduce vector infectivity. However, vectors PEGylated with 20K PEG barely transduced cells (for representative data see Fig. 1d). Results were confirmed with Hepa1–6 cells, which are of murine origin (data not shown). The data demonstrated that position-specific capsid modification with only ~700 molecules can maintain vector infectivity (5K-PEG) even though it significantly changed the charge and size of particles. This is in contrast to earlier approaches that involved up to 14,000 modification sites per particle [32,34,35].

3.2. Ablation of FX-binding by minimal geneti-chemical modification

Surface plasmon resonance (SPR) analysis was performed to analyze binding of unPEGylated and PEGylated Ad-HVR1 and Ad-HVR1-ΔFX vector particles to FX (Figs. 2a and S1). UnPEGylated Ad-HVR1 vector particles bound to FX to an extent similar to Ad-wtcapsid particles (rel. response units (RU) in %: 93.5 ± 7.0%). UnPEGylated Ad-HVR1-ΔFX vectors, however, showed a significantly reduced binding to FX (rel. RU in %: 17.2 ± 0.6%), which is in agreement with work by Alba et al. [28]. PEGylated Ad-HVR1 vector particles exhibited reduced binding to FX in a PEG size-dependent manner (rel. RU in %: 2K-PEG: 38.9 ± 1.9%; 5K-PEG: 7.7 ± 0.8%; 20K-PEG: 3.3 ± 0.8%). Interestingly, PEGylation of Ad-HVR1-ΔFX vectors, *i.e.* the combination of the ΔFX mutation with PEGylation of HVR1, decreased binding to FX to baseline (rel. RU in %: 2K-PEG: 5.9 ± 0.3%; 5K-PEG: 4.7 ± 0.7%; 20-PEG: 5.5 ± 1.5%).

Transduction assays were performed to assess biological effects of altered FX-binding *in vitro* (Fig. 2b, supplementary info for the assay in Fig. S2). To exclude a CAR-mediated transduction, ΔCAR vectors were used. The presence of physiological concentrations of FX augmented the transduction by unPEGylated, 2K-, and 5K-PEGylated Ad-HVR1-ΔCAR vectors, which was in agreement to the biophysical data obtained by SPR analysis. Surprisingly, the vector 2K-PEG-Ad-HVR1-ΔCAR exhibited a very strong transduction in the presence of FX, which was corroborated in SKOV-3 cells (Fig. S3). In contrast, unPEGylated and 2K-PEGylated Ad-HVR1-ΔCAR-ΔFX vectors showed only a modestly enhanced transduction of cells in the presence of FX. 5K-PEG-Ad-HVR1-ΔCAR-ΔFX vectors did not show augmented transduction of cells in the presence of FX and 20K-PEGylated Ad-HVR1-ΔCAR and 20K-PEGylated Ad-HVR1-ΔCAR-ΔFX vector particles did not transduce cells at all. These biological *in vitro* assays complemented the results of the SPR analysis: thiol-directed PEGylation of HVR1 reduced FX-binding in a PEG size-dependent manner. 5K-PEGylation of HVR1 in combination with a ΔFX mutation resulted in undetectable binding to FX and ablated its biological effects *in vitro* but maintained vector infectivity *per se*. Vector particles PEGylated with 20K-PEG at HVR1 did not bind to FX but lost infectivity.

3.3. FX-independent hepatocyte transduction by PEGylated vectors in vivo

FX plays an important role for hepatocyte transduction by adenovirus type 5 *in vivo* [12,13]. Since the modified vectors showed a reduced (2K- and 5K-PEGylated Ad-HVR1, unPEGylated and 2K-PEGylated Ad-HVR1-ΔFX, Fig. 2a) or completely ablated FX-binding (20K-PEGylated Ad-HVR1, 5K- and 20K-PEGylated Ad-HVR1-ΔFX, Fig. 2a) we analyzed their capacity to transduce hepatocytes *in vivo*. 2×10^{10} VP were injected into the tail vein of BALB/c mice and the EGFP expression level in liver homogenates was quantified 72 h p.i. by fluorometic analysis (Fig. 3a). EGFP expression levels in liver were comparable after injection of unPEGylated Ad-HVR1-ΔCAR and the control vector Ad-wtcapsid. In contrast, only background fluorescence levels were detected after injection of unPEGylated Ad-HVR1-ΔCAR-ΔFX. Surprisingly, highest EGFP expression levels were detected in livers after injection of 2K-PEGylated Ad-HVR1-ΔCAR or 2K- and 5K-PEGylated Ad-HVR1-ΔCAR-ΔFX vectors (compared to unPEGylated counterparts: 2K-PEG-Ad-HVR1-ΔCAR: 35-fold increase, $p < 0.006$; 2K-PEG-Ad-HVR1-ΔCAR-ΔFX: 60-fold increase, $p < 3.7 \times 10^{-8}$; 5K-PEG-Ad-HVR1-ΔCAR-ΔFX: 177-fold increase, $p < 0.003$). Of note, the EGFP expression in liver mediated by 5K-PEG-Ad-HVR1-ΔCAR-ΔFX did apparently not depend on FX (Fig. 3a). 20K-PEGylated vectors did not transduce the liver.

To confirm the results obtained by fluorometic analysis, liver cryosections were prepared and EGFP expression was analyzed in direct fluorescence images (Fig. 3b). The results corroborated increased transduction levels (Fig. 3a) and suggested hepatocytes being the mainly

Table 1
Overview of generated mutant Ad5 vectors.

Vector designation	Modification		
	cysteine within HVR1 [36]	CAR-binding inhibited [37]	FX-binding inhibited [28]
Ad-wtcapsid	–	–	–
Ad-HVR1	●	–	–
Ad-HVR1-ΔCAR	●	●	–
Ad-HVR1-ΔFX	●	–	●
Ad-HVR1-ΔCAR-ΔFX	●	●	●

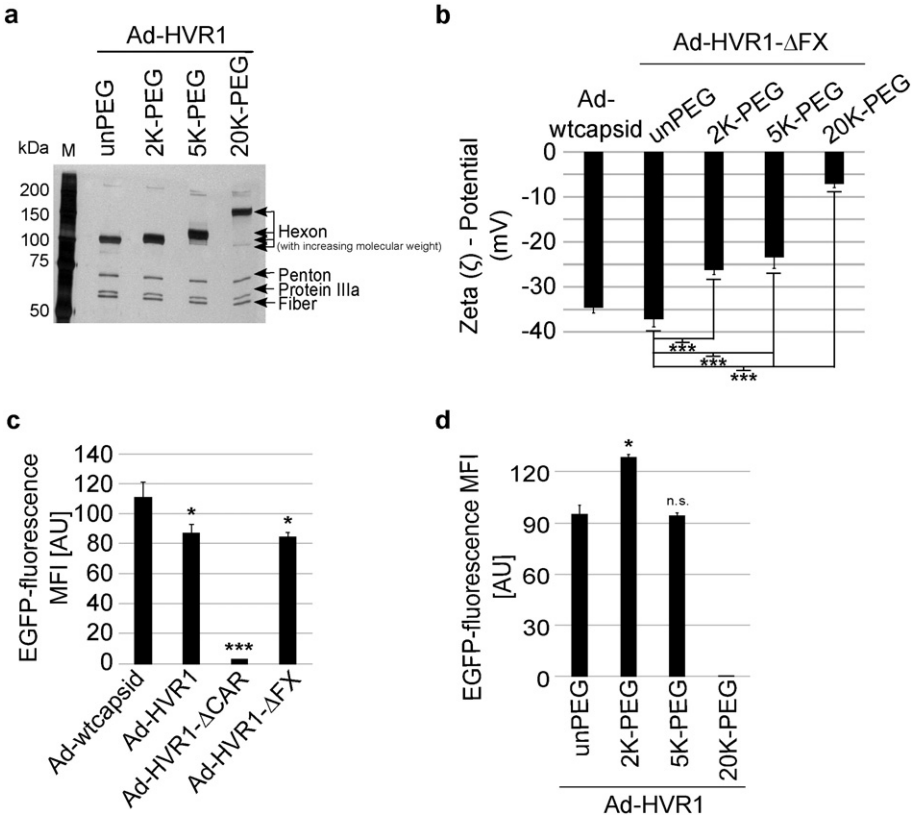

Fig. 1. Near quantitative position-specific PEGylation of HVR1 reduced the negative surface charge of Ad5 particles but maintained vector infectivity with PEG ≤ 5 kDa. (a) Silver staining of 1×10^{10} VP PEGylated or unPEGylated Ad-HVR1 vector particles, separated on an 8% SDS-PAGE under denaturing conditions. PEG size-dependent increase of the molecular weight of the monomeric hexon. M: marker (b) Surface charge of Ad-wtcapsid and unPEGylated or PEGylated vector particles analyzed by ZetaPotential measurements (n = 5). (c) Transduction assay using Ad-wtcapsid, Ad-HVR1, Ad-HVR1-ΔCAR, and Ad-HVR1-ΔFX. A549 cells were transduced with pMOI 1000, harvested 24 h p.i. and EGFP expression was analyzed by flow cytometry (n = 3). (d) Transduction assay using PEGylated Ad-HVR1 vectors. A549 cells were transduced with pMOI 1000, harvested 24 h p.i. and EGFP expression was analyzed by flow cytometry (n = 3). Results are given as mean ± standard deviation. MFI: mean fluorescence intensity, AU: arbitrary units, unPEG: unPEGylated, *p ≤ 0.05,**p ≤ 0.005, ***p ≤ 0.0005.

transduced cell type. Cryo-sections of spleens revealed a slightly augmented transduction of spleen cells by vectors PEGylated with 2K- or 5K-PEG compared to control or unPEGylated vectors (Fig. 3b). 20K-PEG-Ad-HVR1-ΔCAR-ΔFX vectors did not transduce the spleen.

In brief, the data demonstrated that vector-bound FX is not a strict requirement for liver transduction by Ad5-based vectors.

3.4. PEGylation can substitute FX to prevent vector neutralization by murine natural antibodies and complement

Recently, Xu et al. demonstrated that ablation of FX-binding rendered vector particles susceptible to neutralization by mouse plasma — a process that depends on natural IgM and the classical complement pathway [5]. Therefore, we analyzed the susceptibility of the PEGylated vector particles for neutralization by plasma from Ad-naïve C57BL/6 or *muMT* −/− mice, the latter being deficient in IgG, IgM, and IgA (Fig. 4a). Ad-HVR1 vector particles were only partially neutralized in Ad-naïve C57BL/6 plasma (mean fluorescence intensity (MFI)-value: 92.5). In contrast, Ad-HVR1-ΔFX particles were completely neutralized (MFI-value: 0.98; $p < 1.1 \times 10^{-6}$ compared to Ad-HVR1 in plasma). Importantly, antibody-deficient *muMT* −/− plasma did not neutralize Ad-HVR1-ΔFX particles (MFI-value: 133; $p < 0.001$ compared to Ad-HVR1-ΔFX in C57BL/6 plasma). This data confirmed a natural antibody-dependent neutralization mechanism. Moreover, heat-inactivated C57BL/6 plasma did not neutralize Ad-HVR1-ΔFX vector particles (MFI-value: 97; $p < 7.3 \times 10^{-10}$ compared to non-heated C57BL/6 plasma), indicating a complement-dependent mechanism. This finding is in line with the previous observations by Xu et al. that shielding of Ad5 by FX protects the vector from neutralization by mouse serum [5]. Results were confirmed with plasma from NMRI and BALB/c mice (data not shown).

To assess whether PEGylation of HVR1 could shield the vector particles from neutralization, we performed a neutralization assay over a range of different vector particle/plasma ratios (Fig. 4b). After incubation in PBS (negative control without plasma; data point 0 μl in Fig. 4b) all vectors transduced A549 cells to a similar extent (MFI-values: unPEGylated Ad-HVR1: 162.5 ± 1.3; unPEGylated Ad-HVR1-ΔFX: 189.6 ± 9.5; 2K-PEG-Ad-HVR1-ΔFX: 197.6 ± 3.8; 5K-PEG-Ad-HVR1-ΔFX: 176 ± 6). At the highest vector particle/plasma ratio (data point 1 μl in Fig. 4b) only Ad-HVR1-ΔFX particles were neutralized (MFI-value: 51.6 ± 9.2), presumably due to a lack of the natural FX shield. UnPEGylated Ad-HVR1(MFI-value: 286.3 ± 23.2), 2K-PEG-Ad-HVR1-ΔFX (MFI-value: 307 ± 15.4), and 5K-PEG-Ad-HVR1-ΔFX (MFI-value:355 ± 12.1) even exhibited a higher transduction of cells compared to that of their counterparts incubated in PBS (data point 0 μl, Fig. 4b). Starting at the second highest vector particle/plasma ratio all

Table 2
PEG size-dependent increase of hydrodynamic vector particle diameter upon PEGylation of HVR1. Particle sizes were determined using NanoSight LM10 with Nanoparticle tracking analysis (NTA) software. Ad-wtcapsid and unPEGylated or PEGylated Ad-HVR1 vectors (1.7×10^6 VP/μl) were analyzed. 100 nm Latex beads (1.4×10^6 beads/μl) were used as control. Results are given as mean ± standard deviation of five independent measurements. UnPEG: unPEGylated.

Vector	Modification	Particle size
Latex beads (100 nm)	–	100 ± 0.5 nm
Ad-wtcapsid	unPEG	111 ± 0.2 nm
Ad-HVR1	unPEG	113 ± 0.8 nm
	2K-PEG	116 ± 1.0 nm
	5K-PEG	118 ± 0.8 nm
	20K-PEG	133 ± 0.7 nm

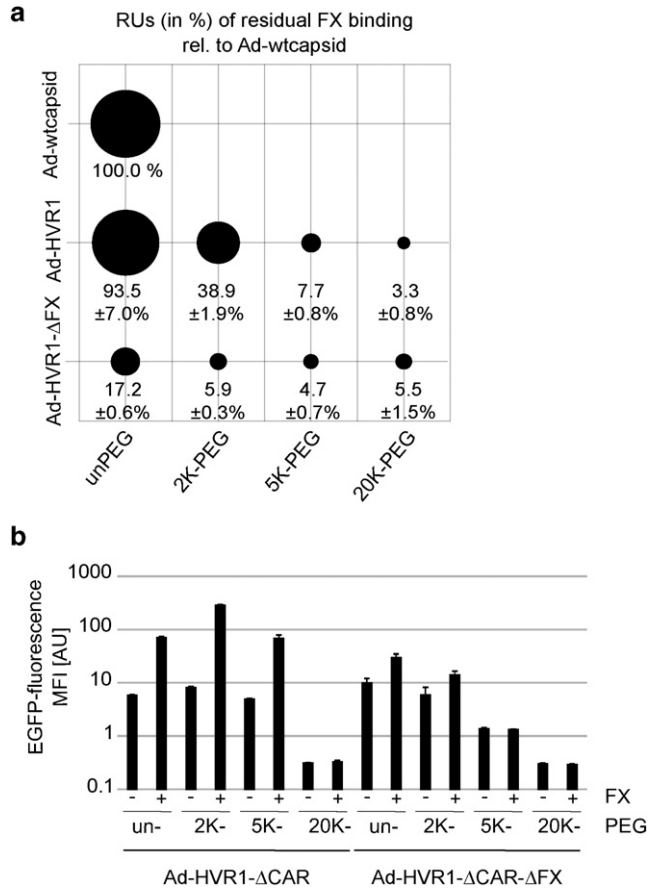

Fig. 2. PEGylation of HVR1 reduced binding of the vector capsid to immobilized FX and eliminated biological effects of FX *in vitro*. (a) Surface plasmon resonance analysis was performed to determine binding of the vector capsid to human FX. Different dilutions of Ad-wtcapsid or PEGylated and unPEGylated Ad-HVR1 and Ad-HVR1-ΔFX vectors (single values or duplicates; ranging from 1×10^9 VP/μl to 6.25×10^7 VP/μl) were injected. Human FX was immobilized on the chip. Since the quality of the FX surface decreased over time, binding of modified vectors to FX was quantified by normalizing the response of modified vectors at concentrations of 1×10^9 VP/μl to the reference Ad-wtcapsid vector (1×10^9 VP/μl), which had been injected immediately before. Circle areas correspond to the percentage of residual FX-binding (n = 2). (b) To measure FX-dependent cell transduction, A549 cells were transduced with pMOI 1000 using unPEGylated or PEGylated Ad-HVR1-ΔCAR and Ad-HVR1-ΔCAR-ΔFX vectors in absence or presence of physiological FX concentrations (8 μg/ml). EGFP expression was analyzed by flow cytometry 24 h p.i. (n = 2). Results are given as mean ± standard deviation. AU: arbitrary units, RU: response units, unPEG: unPEGylated.

particles were neutralized in a plasmaconcentration-dependent manner.

Taken together, the results showed that 2K- or 5K-PEGylated Ad-HVR1-ΔFX vector particles were protected from neutralization at high vector particles/plasma ratios (compare MFI-values of data point 0 μl and data point 1 μl in Fig. 4b). This indicated that position-specific PEGylation of HVR1 successfully replaced the FX-mediated shielding of vector particles from natural antibodies and complement.

3.5. Increased hepatocyte transduction by PEGylated Ad-HVR1-ΔCAR-ΔFX vectors in antibody-deficient mice

Liver transduction by Ad5 vectors is extremely sensitive to inhibition by natural IgM antibodies, especially when the vector is not shielded by FX [5,47–49]. As a result, liver transduction by Ad5 vectors is higher in antibody-deficient mice than in wild-type mice [47,49]. To determine whether increased hepatocyte transduction in BALB/c mice by PEGylated Ad-HVR1-ΔCAR-ΔFX (Fig. 3a) could be completely attributed to avoiding natural antibodies and complement, we examined liver transduction in antibody-deficient J_HD mice. We injected 2×10^{10} particles of unPEGylated or PEGylated Ad-HVR1-ΔCAR-ΔFX vectors *via* the tail vein, and measured EGFP in liver homogenates at 72 h p.i. (Fig. 5). The data showed recovered hepatocyte transduction by unPEGylated Ad-HVR1-ΔCAR-ΔFX in antibody-deficient J_HD mice that was not observed in BALB/c mice (Fig. 3a). This finding of a FX-independent hepatocyte transduction in the absence of natural antibodies is in accordance with findings of Xu et al. [5]. Interestingly, results clearly showed that 2K- and 5K-PEGylated Ad-HVR1-ΔCAR-ΔFX vectors exhibited augmented liver transduction compared to unPEGylated vectors (8-fold, $p < 0.03$; 14-fold, $p < 0.05$, respectively). 20K-PEG-Ad-HVR1-ΔCAR-ΔFX vectors did not transduce hepatocytes.

Thus, improvement in liver transduction by 2K- and 5K-PEG seemed to be attributed to more than only avoiding natural antibodies: 2K- and 5K-PEGylation of Ad-HVR1-ΔCAR-ΔFX vectors had beneficial effects on liver transduction even in mice that completely lacked antibodies.

3.6. PEGylation of HVR1 shielded vector particles from complement

Previously, it was shown *in vivo* that FX is not required for liver transduction in C1q or C4 knockout mice. *In vitro* it has been demonstrated that capsid-bound FX reduces the C3 convertase activity and shields the vector from opsonization by C3 [5]. Since the *in vitro* assays demonstrated that PEGylation of HVR1 substituted a FX-mediated shielding and prevented complement-dependent neutralization of particles in murine plasma (Fig. 4a,b), we analyzed the binding of C3b to PEGylated particles by ELISA. Ad-coated plates were incubated with hirudinized murine plasma that had physiological Ca^{2+} concentrations to allow binding of FX and activation of the classical complement pathway (Fig. 6, left panel). In accordance with literature, results showed enhanced C3b-binding to Ad-HVR1-ΔFX vector particles compared to Ad-HVR1 ($p < 6.7 \times 10^{-8}$). However and interestingly, PEGylation of HVR1 significantly reduced the binding of C3b to the capsid in a PEG size-dependent manner (compared to unPEGylated Ad-HVR1-ΔFX: 2K-PEG: $p < 2.5 \times 10^{-7}$; 5K-PEG: $p < 2.2 \times 10^{-6}$; 20K-PEG: $p < 3.2 \times 10^{-10}$). By the use of an αAd5 fiber antibody, we confirmed equal coating efficiencies for all vectors (Fig. 6, right panel). Thus, PEGylation of HVR1 substituted FX and shielded the vector capsid from opsonization by the complement system.

3.7. PEGylation of HVR1 prevented antibody/complement-mediated uptake of Ad5 by murine macrophages

Xu et al. demonstrated that both natural antibodies and complement contribute to the sequestration of Ad5 vector particles by KC [6]. Since the *in vitro* neutralization assays confirmed that PEGylation of HVR1 had substituted FX-mediated shielding (Figs. 4b and 6), we analyzed the uptake of the geneti-chemically modified vector particles by the murine macrophage cell line Raw264.7 after 2 h incubation. To mimic the *in vivo* situation, the uptake of vector particles was analyzed in the presence of Ad-naïve hirudinized murine plasma. The uptake of vector particles into murine macrophages after incubation in C57BL/6 plasma was increased for Ad-HVR1-ΔFX compared to Ad-HVR1 (7.7-fold; $p < 6.7 \times 10^{-4}$; Fig. 7a). This effect was abolished when vectors were incubated in heat-inactivated plasma ($p < 7.3 \times 10^{-4}$; Fig. 7a) or plasma from antibody-deficient muMT −/− mice (Fig. 7b). This indicated a complement- and natural antibody-dependent uptake mechanism. Importantly, PEGylation largely ablated the uptake of Ad-HVR1-ΔFX vectors (2K-PEG: $p < 0.04$; 5K-PEG: $p < 0.03$; 20K-PEG: $p < 0.002$; Fig. 7c). The results were confirmed with a second murine macrophage cell line J774A.1 (data not shown) and with plasma from NMRI and BALB/c mice (data not shown).

3.8. Improved pharmacokinetics of PEGylated Ad-HVR1-ΔCAR-ΔFX vectors

The uptake of Ad5 by macrophages is an efficient and rapid mechanism [1,8]. To analyze if PEGylated vector particles might exhibit

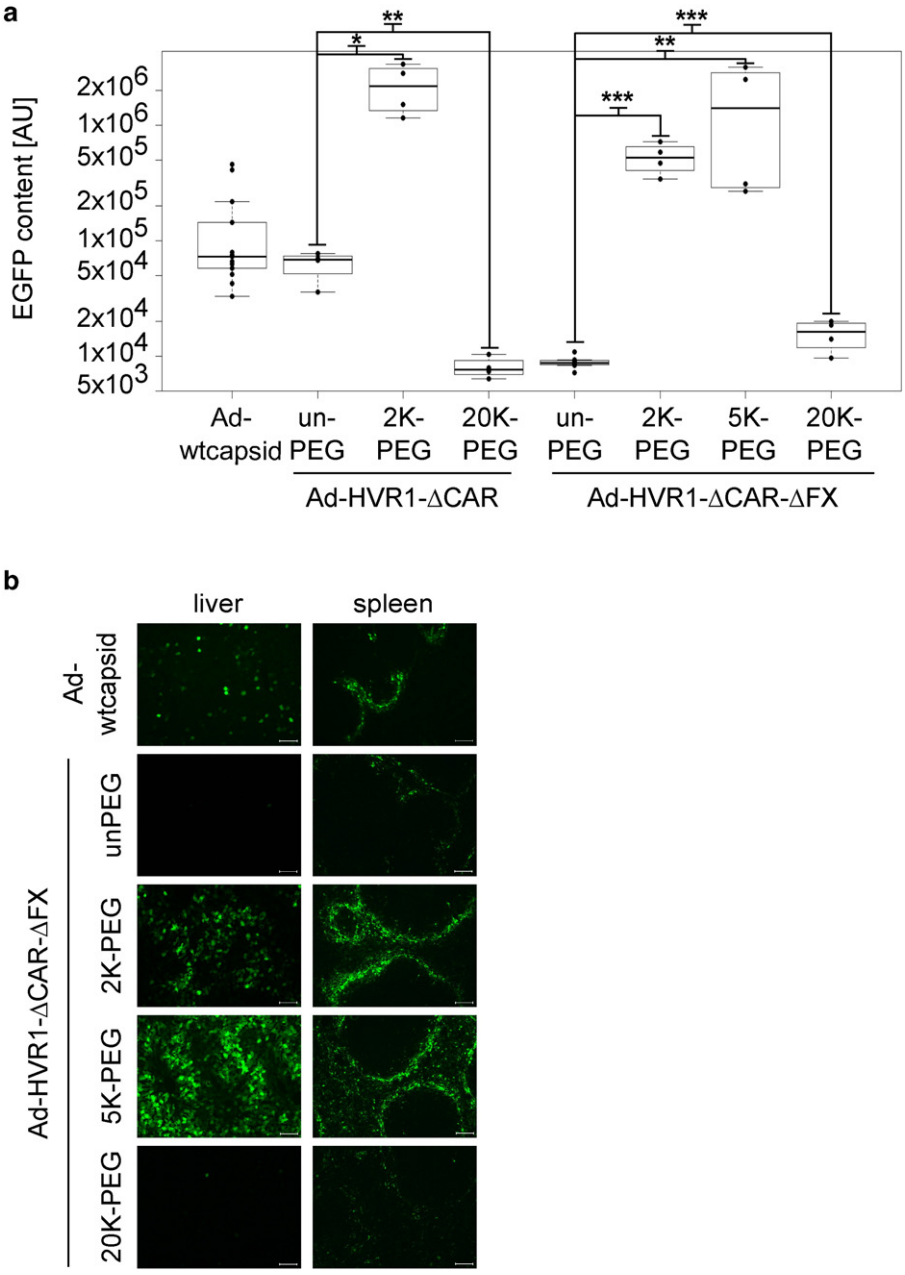

Fig. 3. Increased FX-independent hepatocyte transduction by PEGylated Ad-HVR1-ΔCAR and Ad-HVR1-ΔCAR-ΔFX vectors. (a) 2×10^{10} VP were injected into the tail vein of BALB/c mice. Mice were sacrificed 72 h later and EGFP expression in liver homogenates was measured by fluorometic analysis (n = 4–13). (b) Fluorescence microscopy of EGFP expression in cryosections (6 μm) of liver and spleen. Scale bar = 0.5 mm. AU: arbitrary units, unPEG: unPEGylated, *p ≤ 0.05, **p ≤ 0.005, ***p ≤ 0.0005.

improved pharmacokinetics, we injected 2×10^{10} VP of unPEGylated or PEGylated Ad-HVR1-ΔCAR and Ad-HVR1-ΔCAR-ΔFX vector particles into the tail vein of BALB/c mice and quantified the Ad5 genomes in blood at several time points early after injection by qPCR (Fig. 8a). The control vectors Ad-wtcapsid and Ad-HVR1-ΔCAR, both of which showed normal FX-binding (Fig. 2a), were rapidly cleared from the blood stream within 20 min (AUC: 8.9×10^8 and 1.6×10^9, respectively). Compared to Ad-wtcapsid, unPEGylated Ad-HVR1-ΔCAR-ΔFX vector particles showed a slightly slower clearance from blood (AUC: 2.2×10^9). In contrast, PEGylation of Ad-HVR1-ΔCAR-ΔFX vectors significantly increased the vector circulation in blood in a PEG size-dependent manner (AUC: 2K-PEG: 9.3×10^9; 5K-PEG: 1.3×10^{10}; 20K-PEG: 1.7×10^{10}). 5K- and 20K-PEGylated Ad-HVR1-ΔCAR-ΔFX vector particles were not cleared within the evaluated period of 20 min (for AUC values see Table 3; for p-values see Table S1). Importantly, we demonstrated that 5K- and 20K-PEGylated vector particles were not cell-associated, thus excluded 'hitchhiking' of particles on blood cells, by analyzing the blood cell fraction and the plasma fraction 20 min p.i. separately (Fig. 8b).

To estimate the toxicity of PEGylated vector particles with improved pharmacokinetics, we incubated hirudinized murine whole blood with unPEGylated or PEGylated Ad-HVR1 and Ad-HVR1-ΔFX for 6 h at 37 °C and determined the IL-6 concentration by ELISA. Results clearly revealed that PEGylated Ad-HVR1-ΔFX vector particles did not significantly enhance IL-6 secretion compared to unPEGylated Ad-HVR1-ΔFX or Ad-HVR1 particles (Fig. 8c).

3.9. PEGylation of HVR1 inhibited scavenger receptor-mediated uptake of Ad5 by macrophages

Xu et al. demonstrated that uptake of Ad5 vector particles by macrophages is not only antibody- and complement- but also scavenger

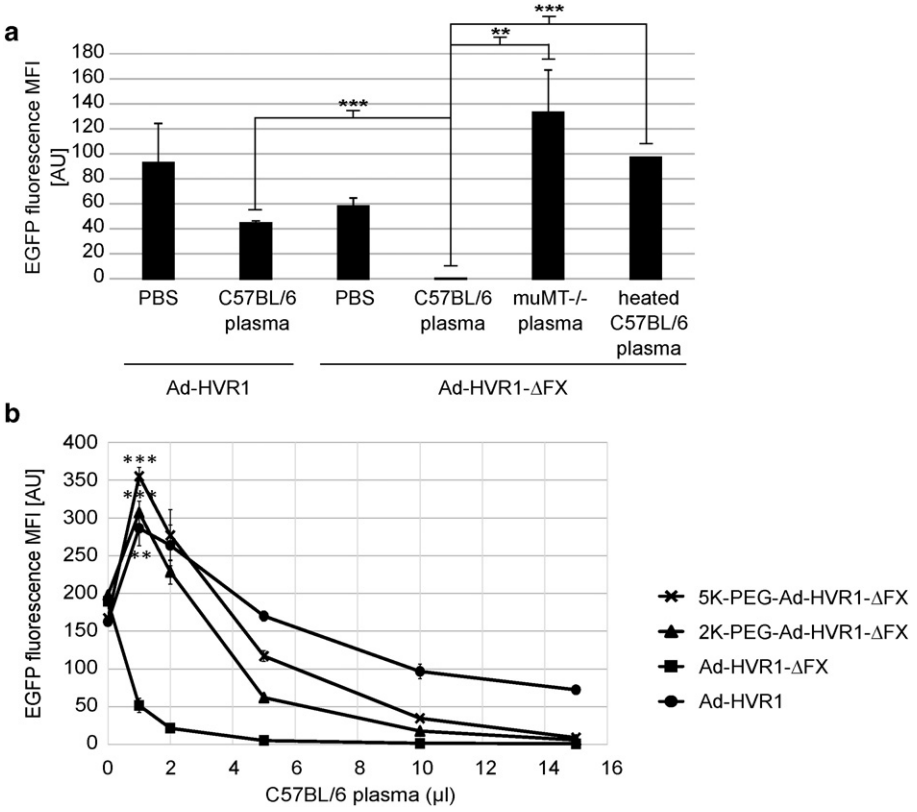

Fig. 4. PEGylation of HVR1 inhibited complement-dependent neutralization of ΔFX vector particles by mouse plasma. (a) Transduction of A549 cells by 2×10^7 VP of Ad-HVR1 and Ad-HVR1-ΔFX vectors (pMOI 1000) in presence of hirudinized C57BL/6 plasma or plasma from antibodies-deficient muMT−/− mice with a vector particle/plasma ratio of 1.3×10^6 VP/µl. To destroy the complement system plasma samples were heated before use at 56 °C for 30 min. Cell transduction was analyzed by measuring the EGFP expression 24 h p.i. (b) Transduction of A549 cells by 2×10^7 VP of unPEGylated Ad-HVR1 and unPEGylated or 2K- and 5K-PEGylated Ad-HVR1-ΔFX (pMOI 1000) after incubation in 1 µl, 2 µl, 5 µl, 10 µl or 15 µl of hirudinized C57BL/6 plasma was analyzed by measuring the EGFP expression 24 h p.i. (n = 3). The vector particle/plasma ratio when using 1 µl plasma corresponded to the vector particle/plasma ratio in the *in vivo* studies. Results are given as mean ± standard deviation. AU: arbitrary units, $^{**}p \le 0.005$, $^{***}p \le 0.0005$.

receptor-mediated [6]. Scavenger receptors can bind negatively charged molecules [22] and the zeta potential analysis (Fig. 1b) had revealed a PEG size-dependent reduction of the negative surface charge for PEGylated particles. Therefore, the scavenging of PEGylated particles was analyzed with the scavenger receptor-expressing cell line J774A.1 [23] in the presence and absence of polyinosinic acid (poly-(I)) as scavenger receptor inhibitor (Fig. 9a). Results clearly demonstrated a scavenger receptor-mediated uptake of unPEGylated Ad-HVR1-ΔFX vector particles, which was 3-fold lower when cells had been pre-treated with poly-(I). PEGylation reduced the uptake of particles by J774A.1 cells in a PEG size-dependent manner (uptake reduction of PEGylated Ad-HVR1-ΔFX particles compared to unPEGylated Ad-HVR1-ΔFX particles: 2K-PEG: 1.7-fold, $p < 0.006$; 5K-PEG: 3-fold, $p < 1.1 \times 10^{-4}$; 20K-PEG: 3.6-fold, $p < 1.3 \times 10^{-4}$). Transduction of scavenger receptor-negative A549 cells by unPEGylated Ad-HVR1-ΔFX vector particles revealed similar EGFP expression levels in absence or presence of poly-(I). Hence poly-(I) did not interfere with vector or cell integrity (Fig. 9b).

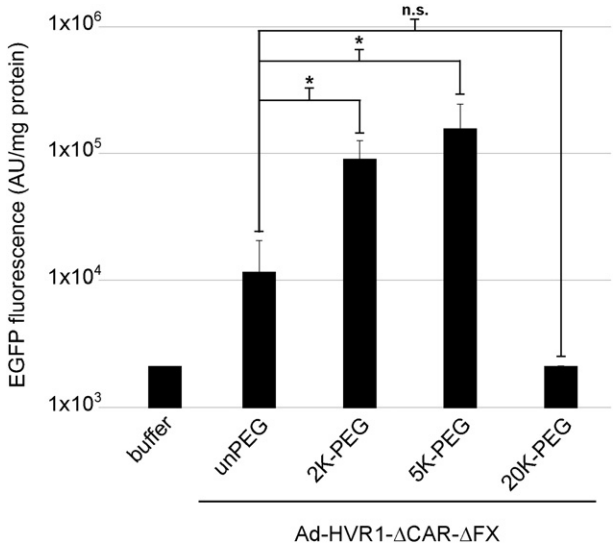

Fig. 5. Increased hepatocyte transduction by PEGylated Ad-HVR1-ΔCAR-ΔFX vectors in antibody-deficient J_HD mice. 2×10^{10} VP were injected into the tail vein of antibody-deficient J_HD mice. Mice were sacrificed 72 h later and EGFP expression in non-perfused liver homogenates was measured by fluorometic analysis (n = 2 for buffer control, n = 3–4 for the vector-treated groups). Results are given as mean ± standard deviation. AU: arbitrary units, unPEG: unPEGylated.

Taken together, position-specific PEGylation diminished antibody- and complement-dependent as well as charge pattern-mediated scavenging by macrophages. Since improved evasion from macrophages can be directly linked to elevated hepatocyte transduction *in vivo* [8,21,23,39], the evasion from macrophages likely contributed to the strong liver transduction *in vivo* (Figs. 3 and 5).

3.10. FX shielded Ad5 from neutralization by naïve human plasma

To our knowledge, FX-mediated shielding from neutralization was so far only shown in mice, guinea pigs and rats [5,26]. To investigate if the effect of a FX-mediated shielding also occurs in human blood, we performed an *in vitro* neutralization assay as described before with hirudinized human plasma from healthy donors (Fig. 10). Prior to the assay, the plasma was tested by ELISA for *anti*-Ad IgGs and classified to be naïve or *anti*-Ad IgG positive. Both Ad-HVR1 and Ad-HVR1-ΔFX

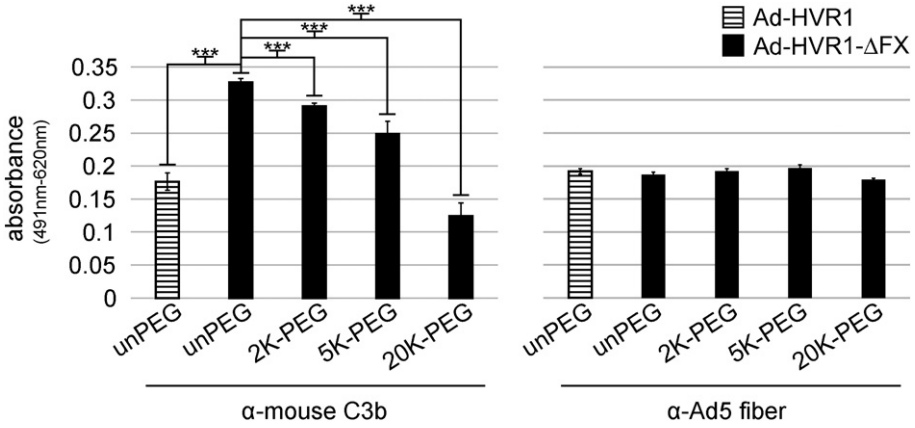

Fig. 6. PEGylation of HVR1 reduced binding of complement protein 3b to the vector capsid. 3×10^9 VP were coated on 96-well plates and were incubated with or without hirudinized murine plasma (diluted 1:5 in PBS with physiological Ca^{2+} concentration) for 1 h. Coating efficiency and binding of C3b to vector capsids was determined by ELISA. Results are given as mean ± standard deviation. (n = 6); unPEG: unPEGylated. ***p ≤ 0.0005.

were completely neutralized using *anti*-Ad IgG-positive plasma (5% EGFP-positive cells; 3% EGFP-positive cells, respectively). In contrast, while Ad-HVR1 was not neutralized by Ad-naïve human plasma (PBS: 80% EGFP-positive cells; plasma: 75% EGFP-positive cells), substantial neutralization was observed for Ad-HVR1-ΔFX in the presence of Ad-naïve human plasma (PBS: 70% EGFP-positive cells; Ad-naïve plasma: 5% EGFP-positive cells, $p < 1.1 \times 10^{-10}$; Ad-HVR1-ΔFX incubated in Ad-naïve plasma compared to Ad-HVR1 incubated in Ad-naïve plasma: $p < 4.1 \times 10^{-8}$). Heat-inactivated Ad-naïve human plasma did not neutralize Ad-HVR1-ΔFX vector particles (85% EGFP-positive cells; compared to non-heated Ad-naïve plasma: $p < 7.6 \times 10^{-11}$). This confirmed a complement-dependent mechanism. Although not directly shown here, it may be possible that besides the obvious role of complement, also natural IgM antibodies contributed to the neutralization of ΔFX vector particles. Thus, data confirmed that the phenomenon of FX-mediated shielding from neutralization in plasma also applies to human blood.

3.11. Binding of ΔFX vectors to human blood cells

Binding of Ad5 to human erythrocytes is mediated either by attachment of the fiber knob to CAR or by αAd IgG-mediated binding to complement receptor 1 (CR1). Both receptors are expressed on human but not murine erythrocytes [14]. To assess whether FX-binding ablation affect attachment of vectors to human blood cells, Ad-HVR1, Ad-HVR1-ΔCAR and Ad-HVR1-ΔCAR-ΔFX vector particles were incubated with hirudinized human whole blood from ELISA-tested Ad-naïve donors. Blood samples were spiked or not spiked with IVIG, a mixture of IgGs purified from pooled human plasma samples and containing αAd5 IgGs [50]. Cell and plasma fractions were separated by centrifugation and the Ad5 genome content was quantified by qPCR (Fig. 11). In agreement to the findings by Carlisle et al. [14] the results revealed for Ad-HVR1 and Ad-HVR1-ΔCAR vector particles a CAR- and IgG-mediated binding to human blood cells, both of which mechanisms resulted in up to 90% cell-associated vector particles (Fig. 11a and b). Incubation of Ad-HVR1 vector particles with ELISA-tested anti-Ad IgG-positive hirudinized human whole blood and subsequent ficoll gradient centrifugation to separate the different blood cell types, confirmed that the vast majority of vector particles bound to erythrocytes (Fig. S4). Interestingly, >75% of Ad-HVR1-ΔCAR-ΔFX vector particles attached to human blood cells after incubation with Ad-naïve human whole blood ($p < 9.3 \times 10^{-11}$ compared to Ad-HVR1-ΔCAR), thus in a CAR- and IgG-independent manner (Fig. 11c). Even though not directly shown here, it may be possible that this binding was mediated by natural antibodies and complement, which bound to the capsids of ΔFX vector particles.

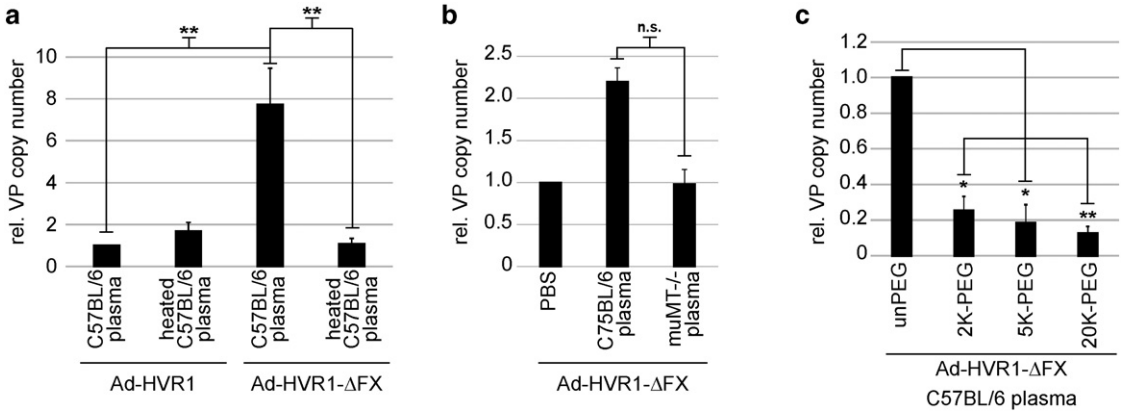

Fig. 7. PEGylation of HVR1 prevented natural antibody- and complement-dependent uptake of ΔFX vector particles by macrophages. Vector particles were incubated in PBS or hirudinized murine plasma in a final concentration of 6×10^6 VP/μl. Subsequently, Raw264.7 cells were incubated with vector:PBS or vector:plasma solution (pMOI 2000) for 2 h at 37 °C. The uptake of Ad5 was measured by qPCR analysis. All samples were normalized using murine β-*actin* copy numbers. (a) Ad-HVR1 and Ad-HVR1-ΔFX vectors were incubated in C57BL/6 plasma. To destroy the complement system plasma samples were heated before use at 56 °C for 30 min. (b) Ad-HVR1-ΔFX vectors were incubated in PBS, plasma from C57BL/6 or plasma from antibody-deficient muMT−/− mice. (c) Ad-HVR1-ΔFX vectors, modified with 2K-, 5K- and 20K-PEG were incubated in C57BL/6 plasma (n = 2–5). Results are given as mean ± standard deviation. UnPEG: unPEGylated. *p ≤ 0.05, **p ≤ 0.005.

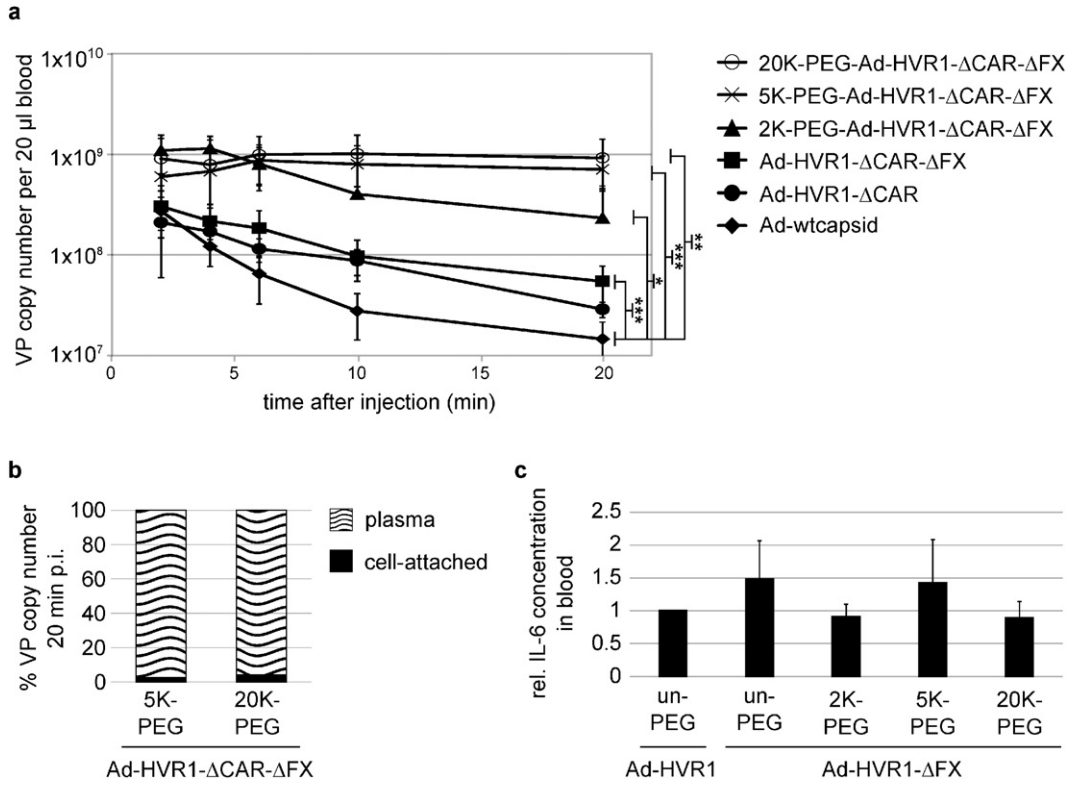

Fig. 8. Improved pharmacokinetics after geneti-chemical Ad capsid modification. (a) The pharmacokinetic profile was determined by injection of 2×10^{10} VP into the tail vein of BALB/c mice and collection of blood samples (20 µl) at distinct time points within 20 min p.i. Genomic DNA was extracted and analyzed for the Ad5 genome copy number by qPCR analysis. (b) 20 min p.i. blood samples (100 µl) were collected by puncturing the heart. Blood cells and plasma were separated by centrifugation, and DNA was extracted from the cell pellet. Results are given as percentage of recovered vector particles in the cell pellet to total recovered vector particles in 20 µl whole blood at 20 min p.i. All samples were normalized using murine β-*actin* copy numbers. Depicted statistic were calculated for Ad5 genome copy numbers compared to Ad-wtcapsid vectors detected after 20 min. Results are given as mean ± standard deviation (n = 3–9). (c) 4×10^9 VP were incubated *ex vivo* with 300 µl hirudinized murine whole blood for 6 h at 37 °C. Plasma was separated by centrifugation for 10 min at 1.000 ×*g* and the IL-6 concentration was determined by ELISA. (n = 3) unPEG: unPEGylated, *p ≤ 0.05, **p ≤ 0.005, ***p ≤ 0.0005.

4. Discussion

Systemic delivery of gene transfer vectors is essential to treat large organ systems or disseminated solid tumors and metastasis. However, gene transfer vectors have to overcome multiple barriers before they can reach their target tissue through the blood stream. Some of these barriers already arise very early upon contact of the vectors with cellular or non-cellular blood components and dictate the fate of the vector particles after systemic delivery. In particular, the clinical utility of Ad5-based vectors is severely hampered by a plethora of such vector-blood interactions. Ad5-based vectors bind blood coagulation factor X [12,13] and this binding controls the tropism of the vector [12,13,28,30]. Simultaneously, complement system, natural antibodies, and macrophages act as innate defense line against pathogens and inactivate Ad5 vectors with remarkable efficiency [1,6,9,10,49]. Noteworthy, interactions between the vector and blood components appear to be very closely intertwined. As a result, Ad vectors rationally engineered to overcome one specific barrier (*e.g.* FX-imposed hepatocyte tropism) may be eliminated by another barrier (*e.g.* complement and natural antibodies) in a sometimes surprising and difficult to predict way [5]. The geneti-chemically modified vectors presented here provide a tool to gain deeper insight into the complex network of Ad5 vector-blood interactions. We demonstrated that binding of FX to Ad5 vector particles is not required for liver transduction. In addition, the pharmacokinetics of systemically delivered Ad5 vectors was significantly improved by rationally selected capsid modifications in combination with minimal position-specific PEG shielding. The data presented here provide significant new insight into how PEGylation improves Ad5 vector properties and suggest that geneti-chemically modified vectors with position-specific PEG shields may be developed into clinically useful therapeutic agents.

Previously, Xu et al. had demonstrated that FX was not required for liver transduction in transgenic mice that lacked antibodies, C1q, or C4 complement components [5]. Since capsid-bound FX protected vector particles from complement and natural antibodies, the authors assigned a shielding function to capsid-bound FX. The data presented here indicate that the shield established by FX can be substituted by PEG moieties coupled to HVR1 of the hexon capsomere. Ad-HVR1-ΔFX specifically PEGylated at HVR1 with 5K-PEG moieties was unable to bind to FX as evidenced by SPR analysis (Fig. 2a), did not exhibit augmented transduction in the presence of FX *in vitro* (Figs. 2b and S3), but transduced liver to an extent even higher than the Ad-wtcapsid vector (Fig. 3a). Importantly, its unPEGylated counterpart Ad-HVR1-ΔFX was susceptible to complement (Fig. 4a) and failed to transduce liver (Fig. 3a). This data proves that approximately 700 PEG moieties coupled to hexon HVR1 established an efficient shield to protect the vector particles from complement and natural antibodies (Figs. 4b and 6) and subsequent uptake by macrophages (Fig. 7). Since PEG as a hydrophilic

Table 3
Increased vector persistence in blood by minimal geneti-chemical modification. Calculation of area under the curve (AUC) between 2 min and 20 min. Results are given as x-fold increase of AUC compared to control vector Ad-wtcapsid. Calculations were done using SciDAVis 1.D5 software. UnPEG: unPEGylated.

	Modification	Increase of AUC rel. to Ad-wtcapsid (x-fold)
Ad-HVR1-ΔCAR-ΔFX	unPEG	2.5
	2K-PEG	10.4
	5K-PEG	15.0
	20K-PEG	19.0

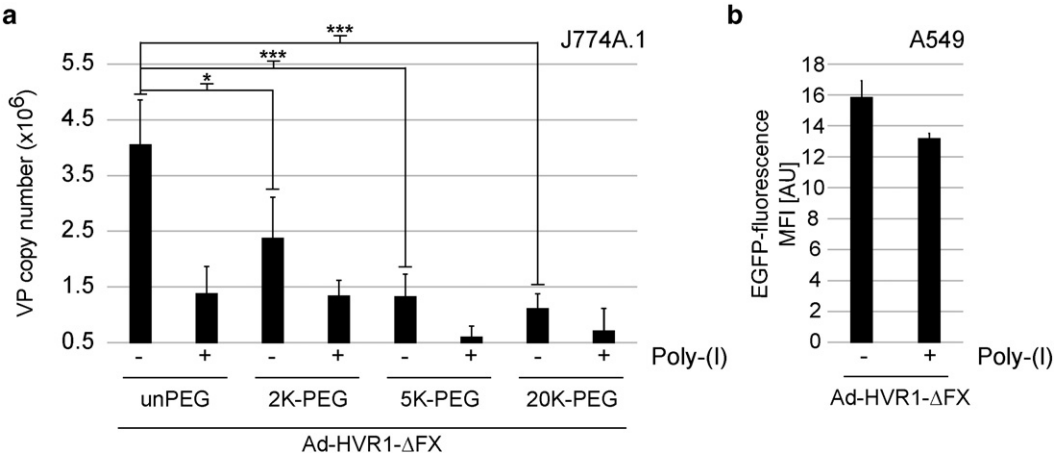

Fig. 9. PEGylation of HVR1 inhibited scavenger receptor-mediated uptake of particles by macrophages. (a) J774A.1 cells were treated or not with 30 μg/ml poly-(I) for 1 h at 37 °C. Subsequently, cells were incubated with unPEGylated and PEGylated Ad-HVR1-ΔFX vector particles (pMOI 2000) for 2 h. Cells were washed and incubated for 24 h at 37 °C. Subsequently, the uptake of Ad5 by the cells was measured by qPCR analysis (n = 6). All samples were normalized using murine β-*actin* copy numbers. (b) A549 were treated or not with 30 μg/ml poly-(I) for 1 h at 37 °C. Subsequently, cells were incubated with Ad-HVR1-ΔFX vector particles (pMOI 1000) for 2 h, washed, and the EGFP expression was analyzed 24 h p.i. by flow cytometry analysis (n = 3). Results are given as mean ± standard deviation. AU: arbitrary units, unPEG: unPEGylated, *p ≤ 0.05, ***p ≤ 0.0005.

inert molecule is not known to have receptor-binding abilities, it remains elusive which receptor was utilized by the PEGylated particles for hepatocyte transduction. Interestingly, Zaiss et al. recently showed that heparan sulfate proteoglycans expressed on the surface of hepatocytes are dispensable for Ad5 liver transduction [51]. In addition, the authors demonstrated that CAR was not responsible for liver transduction in transgenic mice lacking HSPG expression on hepatocytes [51]. These findings are in agreement with and provide complementary information to the results presented here: Ad5 particles can transduce hepatocytes even in the absence of HSPGs [51] when FX provides a shield against complement and natural antibodies [5]. If the shield established by FX on the capsid is substituted by PEG molecules, neither FX- nor CAR-binding are required for liver transduction (Fig. 3a).

Thus, it appears very likely that Ad5 can utilize a so far unknown receptor for liver transduction. Obviously, to fully elucidate the biology of liver transduction by Ad5 (and presumably other types) more research efforts are required.

Our data further suggest that both Ad5 particle charge and size are important parameters that can be modulated by geneti-chemical capsid modifications. While we do not provide direct evidence, our data suggest that reducing the net negative charge of Ad5 particles might facilitate evasion from scavenging by macrophages (Fig. 9a) and enables prolonged circulation of vector particles in blood (Fig. 8a). The data on reduced scavenging is in agreement to findings by Khare et al. for Ad5/6 chimeric vectors with hexon HVRs derived from Ad6 that efficiently evaded from scavenging by Kupffer cells *in vivo* [21,24]. Ad6 has a more neutral net charge compared to Ad5 [24]. Interestingly, we found that vector particles shielded with 2K-PEG or 5K-PEG with a reduced negative net charge (Fig. 1b) exhibited slightly augmented infectivity *in vitro* (Fig. 1d). This finding was corroborated on various cell lines (data not shown). We speculate that the reduced negative charge may facilitate binding to cell surfaces by reducing charge repulsion effects. This may also contribute to the improved liver transduction by 2K- and 5K-PEGylated vectors (Figs. 3a and 5).

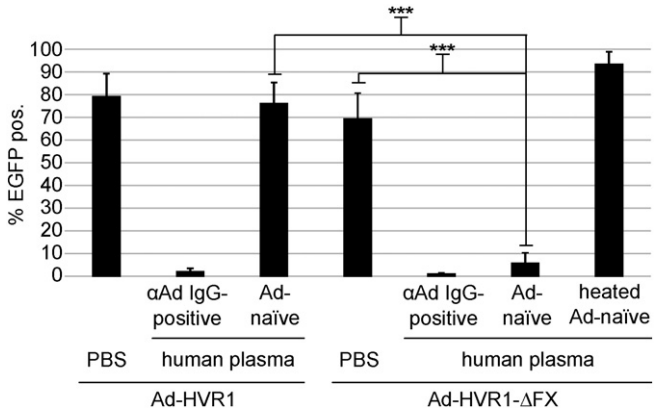

Fig. 10. Neutralization of ΔFX vector particles in Ad-naïve human plasma. Transduction of A549 cells by 2×10^7 VP of Ad-HVR1 and Ad-HVR1-ΔFX vectors (pMOI 1000) in the presence of hirudinized plasma from Ad-naïve or *anti*-Ad IgG-positive human plasma with a vector particles/plasma ratio of 1.3×10^6 VP/μl. To destroy complement system, plasma samples were heated before use at 56 °C for 30 min. Transduction of cells was analyzed by measuring the EGFP expression 24 h p.i. by flow cytometry. Results are given as mean ± standard deviation (n = 5–10). ***p ≤ 0.0005.

Position-specific PEGylation in combination with genetic point mutations significantly reduced the blood clearance of Ad5 vector particles after intravenous vector injection (Fig. 8a). Compared to previous approaches based on amine-directed chemical modification that employed 14,000 amine groups per capsid for polymer coupling [31,35], we achieved similar results by position-specific coupling of only 700 polymer molecules. *Ex vivo* data confirmed that PEGylation did not increase vector toxicity in blood (Fig. 8c). Considering that improved pharmacokinetics might allow for a reduction of the required vector dose, position-specific PEGylation could indirectly contribute to a dampened vector toxicity. 5K-PEG-Ad-HVR1-ΔCAR-ΔFX showed a 19-fold improved AUC between minutes 2 and 20 compared to Ad5 with wildtype capsid. Nevertheless, 72 h after injection the vector particles transduced hepatocytes with high efficiency (Fig. 3a). It will be important to analyze the biodistribution of 5K-PEG-Ad-HVR1(-ΔCAR)-ΔFX particles in tumor models with well-vascularized tumors to assess if the improved pharmacokinetics, as observed here, is sufficient to accumulate the vector particles in tumors *via* the enhanced permeability and retention effect [52]. In parallel, an identification of the so far unknown receptor for liver transduction will pave the way for additional vector improvements.

While the infectivity of Ad vector particles can be impaired in particular by extensive polymer wrapping [32–35], the position-specific coupling of PEG moieties with a size of up to 5K did not diminish vector infectivity (Fig. 1d). In contrast, coupling of 20K-PEG molecules rendered the vector particles non-infectious (Fig. 1d). While the molecular reason for this observation remains unknown, it indicates that successful modification of Ad vector with synthetic polymers depends on careful selection of both the site of modification and the polymer size.

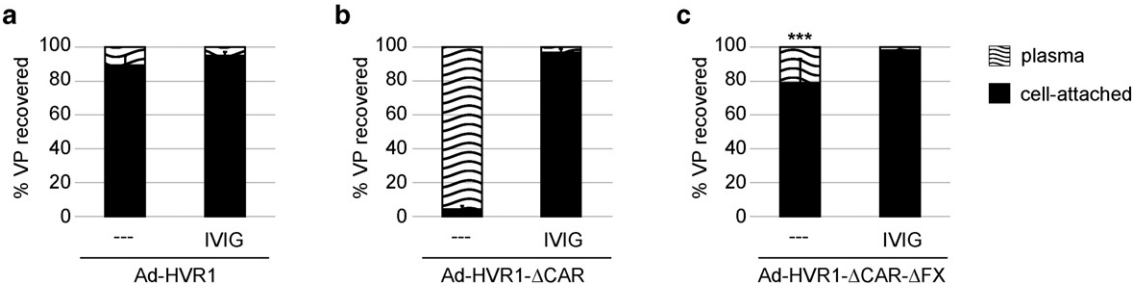

Fig. 11. Binding of ΔFX vectors to human blood cells. 1×10^8 vector particles were incubated with 200 μl hirudinized Ad-naïve human whole blood ± 10 mg/ml of human IgG (IVIG) in a final volume of 300 μl for 30 min at 37 °C. Blood cells and plasma were separated by centrifugation, followed by genomic DNA extraction and analysis of the Ad5 content by qPCR. Results are given as mean percentage ± standard deviation of recovered vector particles from total recovered vector particles in both the cell and plasma fraction. Ad5 DNA copy number was normalized using human β-actin copy numbers. (a) Ad-HVR1 vector (n = 6). (b) Ad-HVR1-ΔCAR vector (n = 9). (c) Ad-HVR1-ΔCAR-ΔFX vector (n = 6–8). ***$p < 0.0005$.

Previous data suggest that restrictions imposed by the size of the coupled polymer can be circumvented by choosing a bioresponsive coupling mode that allows the separation of polymer and vector particles after cell entry [44,53]. Such techniques can easily be applied for the vectors presented here [44].

Finally, our data emphasize the importance of extensive analysis of vector-blood interactions to understand barriers for gene delivery on a cellular and molecular level. While most of the data presented here were obtained by using mice and mouse blood, we also provide hints that the findings can be transferred to humans. The data demonstrate that capsid-bound FX can shield Ad5 particles from human blood components, namely complement (Fig. 10). In addition, we demonstrated that inhibition of FX-binding to vector capsids resulted in increased binding of particles to human blood cells (Fig. 11c). In agreement with the mouse data, this demonstrates the need to substitute the natural FX shield by a rationally designed synthetic shield - in order to enhance vector maintenance and improve the clinical applicability of Ad5 and presumably other Ad-based vectors.

Acknowledgement

This work was supported by the International Graduate School Ulm (IGradU, Excellence Initiative of the German Federal and State Governments) and the German Federal Ministry of Education and Research (BMBF, EXIST Forschungstransfer, 03EFEBW084, BMBF GO-Bio 0315562). We thank Moritz Krutzke for design and realization of the graphical abstract.

Appendix A. Supplementary data

Supplementary data to this article can be found online at http://dx.doi.org/10.1016/j.jconrel.2016.06.022.

References

[1] L.P. Ganesan, S. Mohanty, J. Kim, K.R. Clark, J.M. Robinson, C.L. Anderson, Rapid and efficient clearance of blood-borne virus by liver sinusoidal endothelium, PLoS Pathog. 7 (2011), http://dx.doi.org/10.1371/journal.ppat.1002281.
[2] D.H. Barouch, M.G. Pau, J.H.H.V. Custers, W. Koudstaal, S. Kostense, M.J.E. Havenga, D.M. Truitt, S.M. Sumida, M.G. Kishko, J.C. Arthur, B. Korioth-Schmitz, M.H. Newberg, D.A. Gorgone, M.A. Lifton, D.L. Panicali, G.J. Nabel, N.L. Letvin, J. Goudsmit, Immunogenicity of recombinant adenovirus serotype 35 vaccine in the presence of pre-existing anti-Ad5 immunity, J. Immunol. 172 (2004) 6290–6297, http://dx.doi.org/10.4049/jimmunol.172.10.6290.
[3] T.C. Mast, L. Kierstead, S.B. Gupta, A.A. Nikas, E.G. Kallas, V. Novitsky, B. Mbewe, P. Pitisuttithum, M. Schechter, E. Vardas, N.D. Wolfe, M. Aste-Amezaga, D.R. Casimiro, P. Coplan, W.L. Straus, J.W. Shiver, International epidemiology of human pre-existing adenovirus (Ad) type-5, type-6, type-26 and type-36 neutralizing antibodies: correlates of high Ad5 titers and implications for potential HIV vaccine trials, Vaccine 28 (2010) 950–957, http://dx.doi.org/10.1016/j.vaccine.2009.10.145.
[4] K.L. Molnar-Kimber, D.H. Sterman, M. Chang, E.H. Kang, M. ElBash, M. Lanuti, A. Elshami, K. Gelfand, J.M. Wilson, L.R. Kaiser, S.M. Albelda, Impact of preexisting and induced humoral and cellular immune responses in an adenovirus-based gene therapy phase I clinical trial for localized mesothelioma, Hum. Gene Ther. 9 (1998) 2121–2133, http://dx.doi.org/10.1089/hum.1998.9.14-2121.
[5] Z. Xu, Q. Qiu, J. Tian, J.S. Smith, G.M. Conenello, T. Morita, A.P. Byrnes, Coagulation factor X shields adenovirus type 5 from attack by natural antibodies and complement, Nat. Med. 19 (2013) 452–457, http://dx.doi.org/10.1038/nm.3107.
[6] Z. Xu, J. Tian, J.S. Smith, A.P. Byrnes, Clearance of adenovirus by Kupffer cells is mediated by scavenger receptors, natural antibodies, and complement, J. Virol. 82 (2008) 11705–11713, http://dx.doi.org/10.1128/JVI.01320-08.
[7] D.M. Shayakhmetov, A. Gaggar, S. Ni, Z.-Y. Li, A. Lieber, Adenovirus binding to blood factors results in liver cell infection and hepatotoxicity, J. Virol. 79 (2005) 7478–7491, http://dx.doi.org/10.1128/JVI.79.12.7478-7491.2005.
[8] R. Alemany, K. Suzuki, D.T. Curiel, Blood clearance rates of adenovirus type 5 in mice, J. Gen. Virol. 81 (2000) 2605–2609.
[9] E. Manickan, J.S. Smith, J. Tian, T.L. Eggerman, J.N. Lozier, J. Muller, A.P. Byrnes, Rapid Kupffer cell death after intravenous injection of adenovirus vectors, Mol. Ther. 13 (2006) 108–117, http://dx.doi.org/10.1016/j.ymthe.2005.08.007.
[10] G. Schiedner, S. Hertel, M. Johnston, V. Dries, N. van Rooijen, S. Kochanek, Selective depletion or blockade of Kupffer cells leads to enhanced and prolonged hepatic transgene expression using high-capacity adenoviral vectors, Mol. Ther. 7 (2003) 35–43.
[11] J. Snoeys, G. Mertens, J. Lievens, T. van Berkel, D. Collen, E.A.L. Biessen, B. De Geest, Lipid emulsions potently increase transgene expression in hepatocytes after adenoviral transfer, Mol. Ther. 13 (2006) 98–107, http://dx.doi.org/10.1016/j.ymthe.2005.06.477.
[12] A.L. Parker, S.N. Waddington, C.G. Nicol, D.M. Shayakhmetov, S.M. Buckley, L. Denby, G. Kemball-Cook, S. Ni, A. Lieber, J.H. McVey, S.A. Nicklin, A.H. Baker, Multiple vitamin K-dependent coagulation zymogens promote adenovirus-mediated gene delivery to hepatocytes, Blood 108 (2006) 2554–2561, http://dx.doi.org/10.1182/blood-2006-04-008532.
[13] S.N. Waddington, J.H. McVey, D. Bhella, A.L. Parker, K. Barker, H. Atoda, R. Pink, S.M.K. Buckley, J.A. Greig, L. Denby, J. Custers, T. Morita, I.M.B. Francischetti, R.Q. Monteiro, D.H. Barouch, N. van Rooijen, C. Napoli, M.J.E. Havenga, S.A. Nicklin, A.H. Baker, Adenovirus serotype 5 hexon mediates liver gene transfer, Cell 132 (2008) 397–409, http://dx.doi.org/10.1016/j.cell.2008.01.016.
[14] R.C. Carlisle, Y. Di, A.M. Cerny, A.F.-P. Sonnen, R.B. Sim, N.K. Green, V. Subr, K. Ulbrich, R.J.C. Gilbert, K.D. Fisher, R.W. Finberg, L.W. Seymour, Human erythrocytes bind and inactivate type 5 adenovirus by presenting Coxsackie virus-adenovirus receptor and complement receptor 1, Blood 113 (2009) 1909–1918, http://dx.doi.org/10.1182/blood-2008-09-178459.
[15] G. Cichon, S. Boeckh-Herwig, D. Kuemin, C. Hoffmann, H.H. Schmidt, E. Wehnes, W. Haensch, U. Schneider, U. Eckhardt, R. Burger, P. Pring-Akerblom, Titer determination of Ad5 in blood: a cautionary note, Gene Ther. 10 (2003) 1012–1017, http://dx.doi.org/10.1038/sj.gt.3301961.
[16] E. Seiradake, D. Henaff, H. Wodrich, O. Billet, M. Perreau, C. Hippert, F. Mennechet, G. Schoehn, H. Lortat-Jacob, H. Dreja, S. Ibanes, V. Kalatzis, J.P. Wang, R.W. Finberg, S. Cusack, E.J. Kremer, The cell adhesion molecule "CAR" and sialic acid on human erythrocytes influence adenovirus in vivo biodistribution, PLoS Pathog. 5 (2009), http://dx.doi.org/10.1371/journal.ppat.1000277.
[17] H.J. Haisma, J.A.A.M. Kamps, G.K. Kamps, J.A. Plantinga, M.G. Rots, A.R. Bellu, Polyinosinic acid enhances delivery of adenovirus vectors in vivo by preventing sequestration in liver macrophages, J. Gen. Virol. 89 (2008) 1097–1105, http://dx.doi.org/10.1099/vir.0.83495-0.
[18] A. Lieber, C.Y. He, L. Meuse, D. Schowalter, I. Kirillova, B. Winther, M.A. Kay, The role of Kupffer cell activation and viral gene expression in early liver toxicity after infusion of recombinant adenovirus vectors, J. Virol. 71 (1997) 8798–8807.
[19] Y. Zhang, N. Chirmule, G.P. Gao, R. Qian, M. Croyle, B. Joshi, J. Tazelaar, J.M. Wilson, Acute cytokine response to systemic adenoviral vectors in mice is mediated by dendritic cells and macrophages, Mol. Ther. 3 (2001) 697–707, http://dx.doi.org/10.1006/mthe.2001.0329.
[20] G. Wolff, S. Worgall, N. van Rooijen, W.R. Song, B.G. Harvey, R.G. Crystal, Enhancement of in vivo adenovirus-mediated gene transfer and expression by prior depletion of tissue macrophages in the target organ, J. Virol. 71 (1997) 624–629.
[21] R. Khare, V.S. Reddy, G.R. Nemerow, M.A. Barry, Identification of adenovirus serotype 5 hexon regions that interact with scavenger receptors, J. Virol. 86 (2012) 2293–2301, http://dx.doi.org/10.1128/JVI.05760-11.
[22] S. Mukhopadhyay, S. Gordon, The role of scavenger receptors in pathogen recognition and innate immunity, Immunobiology 209 (2004) 39–49, http://dx.doi.org/10.1016/j.imbio.2004.02.004.

[23] P. Piccolo, F. Vetrini, P. Mithbaokar, N.C. Grove, T. Bertin, D. Palmer, P. Ng, N. Brunetti-Pierri, SR-A and SREC-I are Kupffer and endothelial cell receptors for helper-dependent adenoviral vectors, Mol. Ther. 21 (2013) 767–774, http://dx.doi.org/10.1038/mt.2012.287.
[24] R. Khare, S.M. May, F. Vetrini, E.A. Weaver, D. Palmer, A. Rosewell, N. Grove, P. Ng, M.A. Barry, Generation of a Kupffer cell-evading adenovirus for systemic and liver-directed gene transfer, Mol. Ther. 19 (2011) 1254–1262, http://dx.doi.org/10.1038/mt.2011.71.
[25] J.O. Konz, R.C. Livingood, A.J. Bett, A.R. Goerke, M.E. Laska, S.L. Sagar, Serotype specificity of adenovirus purification using anion-exchange chromatography, Hum. Gene Ther. 16 (2005) 1346–1353, http://dx.doi.org/10.1089/hum.2005.16.1346.
[26] J. Ma, M.R. Duffy, L. Deng, R.S. Dakin, T. Uil, J. Custers, S.M. Kelly, J.H. McVey, S.A. Nicklin, A.H. Baker, Manipulating adenovirus hexon hypervariable loops dictates immune neutralisation and coagulation factor X-dependent cell interaction in vitro and in vivo, PLoS Pathog. 11 (2015) e1004673, http://dx.doi.org/10.1371/journal.ppat.1004673.
[27] M.A. Croyle, Q.-C. Yu, J.M. Wilson, Development of a rapid method for the PEGylation of adenoviruses with enhanced transduction and improved stability under harsh storage conditions, Hum. Gene Ther. 11 (2000) 1713–1722, http://dx.doi.org/10.1089/10430340050111368.
[28] R. Alba, A.C. Bradshaw, A.L. Parker, D. Bhella, S.N. Waddington, S.A. Nicklin, N. van Rooijen, J. Custers, J. Goudsmit, D.H. Barouch, J.H. McVey, A.H. Baker, Identification of coagulation factor (F)X binding sites on the adenovirus serotype 5 hexon: effect of mutagenesis on FX interactions and gene transfer, Blood 114 (2009) 965–971, http://dx.doi.org/10.1182/blood-2009-03-208835.
[29] A.C. Bradshaw, A.L. Parker, M.R. Duffy, L. Coughlan, N. van Rooijen, V.-M. Kähäri, S.A. Nicklin, A.H. Baker, Requirements for receptor engagement during infection by adenovirus complexed with blood coagulation factor X, PLoS Pathog. 6 (2010) e1001142, http://dx.doi.org/10.1371/journal.ppat.1001142.
[30] R. Alba, A.C. Bradshaw, L. Coughlan, L. Denby, R.A. McDonald, S.N. Waddington, S.M.K. Buckley, J.A. Greig, A.L. Parker, A.M. Miller, H. Wang, A. Lieber, N. van Rooijen, J.H. McVey, S.A. Nicklin, A.H. Baker, Biodistribution and retargeting of FX-binding ablated adenovirus serotype 5 vectors, Blood 116 (2010) 2656–2664, http://dx.doi.org/10.1182/blood-2009-12-260026.
[31] N.K. Green, C.W. Herbert, S.J. Hale, A.B. Hale, V. Mautner, R. Harkins, T. Hermiston, K. Ulbrich, K.D. Fisher, L.W. Seymour, Extended plasma circulation time and decreased toxicity of polymer-coated adenovirus, Gene Ther. 11 (2004) 1256–1263, http://dx.doi.org/10.1038/sj.gt.3302295.
[32] C.R. O'Riordan, A. Lachapelle, C. Delgado, V. Parkes, S.C. Wadsworth, A.E. Smith, G.E. Francis, PEGylation of adenovirus with retention of infectivity and protection from neutralizing antibody in vitro and in vivo, Hum. Gene Ther. 10 (1999) 1349–1358, http://dx.doi.org/10.1089/10430349950018021.
[33] A. Wortmann, S. Vöhringer, T. Engler, S. Corjon, R. Schirmbeck, J. Reimann, S. Kochanek, F. Kreppel, Fully detargeted polyethylene glycol-coated adenovirus vectors are potent genetic vaccines and escape from pre-existing anti-adenovirus antibodies, Mol. Ther. 16 (2008) 154–162, http://dx.doi.org/10.1038/sj.mt.6300306.
[34] H. Mok, D.J. Palmer, P. Ng, M.A. Barry, Evaluation of polyethylene glycol modification of first-generation and helper-dependent adenoviral vectors to reduce innate immune responses, Mol. Ther. 11 (2005) 66–79, http://dx.doi.org/10.1016/j.ymthe.2004.09.015.
[35] K.D. Fisher, Y. Stallwood, N.K. Green, K. Ulbrich, V. Mautner, L.W. Seymour, Polymer-coated adenovirus permits efficient retargeting and evades neutralising antibodies, Gene Ther. 8 (2001) 341–348, http://dx.doi.org/10.1038/sj.gt.3301389.
[36] F. Kreppel, J. Gackowski, E. Schmidt, S. Kochanek, Combined genetic and chemical capsid modifications enable flexible and efficient de- and retargeting of adenovirus vectors, Mol. Ther. 12 (2005) 107–117, http://dx.doi.org/10.1016/j.ymthe.2005.03.006.
[37] I. Kirby, E. Davison, A.J. Beavil, C.P.C. Soh, T.J. Wickham, P.W. Roelvink, I. Kovesdi, B.J. Sutton, G. Santis, Identification of contact residues and definition of the CAR-binding site of adenovirus type 5 fiber protein, J. Virol. 74 (2000) 2804–2813, http://dx.doi.org/10.1128/JVI.74.6.2804-2813.2000.
[38] G. Schiedner, S. Hertel, S. Kochanek, Efficient transformation of primary human amniocytes by E1 functions of Ad5: generation of new cell lines for adenoviral vector production, Hum. Gene Ther. 11 (2000) 2105–2116, http://dx.doi.org/10.1089/104303400750001417.
[39] J.-M. Prill, S. Espenlaub, U. Samen, T. Engler, E. Schmidt, F. Vetrini, A. Rosewell, N. Grove, D. Palmer, P. Ng, S. Kochanek, F. Kreppel, Modifications of adenovirus hexon allow for either hepatocyte detargeting or targeting with potential evasion from Kupffer cells, Mol. Ther. 19 (2011) 83–92, http://dx.doi.org/10.1038/mt.2010.229.
[40] J.V. Maizel Jr., D.O. White, M.D. Scharff, The polypeptides of adenovirus: I. Evidence for multiple protein components in the virion and a comparison of types 2, 7A, and 12, Virology 36 (1968) 115–125, http://dx.doi.org/10.1016/0042-6822(68)90121-9.
[41] F. Kreppel, V. Biermann, S. Kochanek, G. Schiedner, A DNA-based method to assay total and infectious particle contents and helper virus contamination in high-capacity adenoviral vector preparations, Hum. Gene Ther. 13 (2002) 1151–1156, http://dx.doi.org/10.1089/104303402320138934.
[42] H. Blum, H. Beier, H.J. Gross, Improved silver staining of plant proteins, RNA and DNA in polyacrylamide gels, Electrophoresis 8 (1987) 93–99, http://dx.doi.org/10.1002/elps.1150080203.
[43] J. Chen, M. Trounstine, F.W. Alt, F. Young, C. Kurahara, J.F. Loring, D. Huszar, Immunoglobulin gene rearrangement in B cell deficient mice generated by targeted deletion of the JH locus, Int. Immunol. 5 (1993) 647–656.
[44] J.-M. Prill, V. Subr, N. Pasquarelli, T. Engler, A. Hoffmeister, S. Kochanek, K. Ulbrich, F. Kreppel, Traceless bioresponsive shielding of adenovirus hexon with HPMA copolymers maintains transduction capacity in vitro and in vivo, PLoS One 9 (2014), http://dx.doi.org/10.1371/journal.pone.0082716.
[45] P. Kramberger, M. Ciringer, A. Strancar, M. Peterka, Evaluation of nanoparticle tracking analysis for total virus particle determination, Virol. J. 9 (2012) 265, http://dx.doi.org/10.1186/1743-422X-9-265.
[46] R Development Core Team, R: A Language and Environment for Statistical Computing, R Foundation for Statistical Computing, Vienna, Austria, 2012 (http://www.R-project.org/).
[47] C. Unzu, I. Melero, A. Morales-Kastresana, A. Sampedro, I. Serrano-Mendioroz, A. Azpilikueta, M.C. Ochoa, J. Dubrot, E. Martinez-Anso, A. Fontanellas, Innate functions of immunoglobulin M lessen liver gene transfer with helper-dependent adenovirus, PLoS One 9 (2014), http://dx.doi.org/10.1371/journal.pone.0085432.
[48] R. Khare, M.L. Hillestad, Z. Xu, A.P. Byrnes, M.A. Barry, Circulating antibodies and macrophages as modulators of adenovirus pharmacology, J. Virol. 87 (2013) 3678–3686, http://dx.doi.org/10.1128/JVI.01392-12.
[49] Q. Qiu, Z. Xu, J. Tian, R. Moitra, S. Gunti, A.L. Notkins, A.P. Byrnes, Impact of natural IgM concentration on gene therapy with adenovirus type 5 vectors, J. Virol. (2014), http://dx.doi.org/10.1128/JVI.03217-14 (JVI.03217-14).
[50] C.A. Chrvala, A. Caspi, Privigen — Immune Globulin Intravenous (Human), 10% Liquid, 2011.
[51] A.K. Zaiss, E.M. Foley, R. Lawrence, L.S. Schneider, H. Hoveida, P. Secrest, A.B. Catapang, Y. Yamaguchi, R. Alemany, D.M. Shayakhmetov, J.D. Esko, H.R. Herschman, Hepatocyte heparan sulfate is required for adeno-associated virus 2 but dispensable for adenovirus 5 liver transduction in vivo, J. Virol. 90 (2015) 412–420, http://dx.doi.org/10.1128/JVI.01939-15.
[52] J. Fang, H. Nakamura, H. Maeda, The EPR effect: unique features of tumor blood vessels for drug delivery, factors involved, and limitations and augmentation of the effect, Adv. Drug Deliv. Rev. 63 (2011) 136–151, http://dx.doi.org/10.1016/j.addr.2010.04.009.
[53] S. Espenlaub, S. Corjon, T. Engler, C. Fella, M. Ogris, E. Wagner, S. Kochanek, F. Kreppel, Capsomer-specific fluorescent labeling of adenoviral vector particles allows for detailed analysis of intracellular particle trafficking and the performance of bioresponsive bonds for vector capsid modifications, Hum. Gene Ther. 21 (2010) 1155–1167, http://dx.doi.org/10.1089/hum.2009.171.